12-2013

EVALUATING THE PREDICTIVE CAPABILITY OF NUMERICAL MODELS CONSIDERING ROBUSTNESS TO NON-PROBABILISTIC UNCERTIANTY IN THE INPUT PARAMETERS

Parker Shields
Clemson University, pshield@g.clemson.edu

EVALUATING THE PREDICTIVE CAPABILITY OF NUMERICAL MODELS CONSIDERING ROBUSTNESS TO NON-PROBABILISTIC UNCERTAINTY IN THE INPUT PARAMETERS

A Thesis
Presented to
the Graduate School of
Clemson University

In Partial Fulfillment
of the Requirements for the Degree
Master of Science
Civil Engineering

---

by
Parker L. Shields
December 2013

Accepted by:
Dr. Sez Atamturktur, Committee Chair
Dr. Abdul Khan
Dr. Hsein Juang
Dr. Scott Cogan

ABSTRACT

The paradigm of model evaluation is challenged by *compensations* between various forms of errors and uncertainties that are inherent to the model development process due to, for instance, imprecise model input parameters, scarcity of experimental data and lack of knowledge regarding an accurate mathematical representation of the system. When calibrating model input parameters based on fidelity to experiments, such compensations lead to non-unique solutions. In turn, the existence of non-unique solutions makes the selection and use of one 'best' numerical model risky. Therefore, it becomes necessary to evaluate model performance based not only on the fidelity of the predictions to experiments but also the model's ability to satisfy fidelity threshold requirements in the face of uncertainties. The level of inherent uncertainty need not be known a priori as the model's predictions can be evaluated for increasing levels of uncertainty, and a model form can be sought that yields the highest probability of satisfying a given fidelity threshold. By implementing these concepts, this manuscript presents a probabilistic formulation of a robust-satisfying approach, along with its associated metric.

This new formulation evaluates the performance of a model form based on the probability that the model predictions match experimental data within a predefined fidelity threshold when subject to uncertainty in their input parameters. This approach can be used to evaluate the robustness and fidelity of a numerical model as part of a model validation campaign, or to compare multiple candidate model forms as part of a model selection campaign. In this thesis, the conceptual framework and mathematical

formulation of this new probabilistic treatment of robust-satisfying approach is presented. The feasibility and application of this new approach is demonstrated on a structural steel frame with uncertain connection parameters, which has undergone static loading conditions.

DEDICATION

I dedicate this thesis to my mom and dad for their unconditional love and support throughout my life, which, at times, I know was not an easy task. I dedicate this thesis to my brother as well, for always looking out for my best interests. I also dedicate this thesis to my loving, late grandparents Earl and Bettie Mease, and Jack and Almeda Shields, who I wish could have witnessed this accomplishment. Without them, I would not have had the opportunities that brought me to where I am today.

ACKNOWLEDGMENTS

I would like to thank my research advisor and committee chair, Dr. Atamturktur, for her valuable guidance and support during my graduate education. I would also like to thank Dr. Juang, Dr. Khan, and Dr. Cogan for their input as my committee members. I would like to thank Eric Michoulier, Ph.D. student at École Nationale Supérieure de Chronométrie et Micromécanique (ENSCM), and his girlfriend, Aurélie Plantureux, for their gracious hospitality as well as collaboration on my thesis during my stay with them in Besançon, France. I am also grateful to Ismail Farajpour, Ph.D. student at Clemson University, and Muxing "Bruce" Ding, M.S. student at Clemson University, for their collaboration with me as well as their intricate contributions to this thesis.

TABLE OF CONTENTS

Page

Table of Contents (Continued)

Page

LIST OF TABLES

LIST OF FIGURES

List of Figures (Continued)

Figure Page

List of Figures (Continued)

Figure Page

CHAPTER ONE

INTRODUCTION

1.1 Motivation

In today's technology driven society, the role of the computer simulation model has become one of utmost importance in the continued success of a majority of the industries that make up the global market. From the design and manufacturing of children's toys to real-time predictions of the ever-fluctuating financial markets to the analysis and design of today's longest and tallest structures, simulation models are at the heart of it all. With the ever-increasing complexity of modern day analytical challenges, the dependence on computer simulations has become inevitable. Therefore, the highest level of confidence in the predictions of these computer models is required to meet the standards of present day practices. Confidence in model predictions can be established through selection of a proper model that can fit the needs of the challenge at hand. Thus, this manuscript presents a novel approach to *model evaluation* that accounts for the uncertainties inherent in the modeling process while evaluating a model's probability of successfully reproducing realistic observations within an accuracy threshold.

In numerical modeling, assumptions often stem from poorly known values of input parameters and lack of knowledge regarding the correct form of equations to characterize the system response behavior. Consequently, numerical models can only provide an approximate representation of the physical reality (Atamturktur et al. 2011), and thus, establishing confidence and credibility in these models' predictions becomes essential for modeling and simulation to support decision making. However, establishing

such confidence is a difficult task when the response of interest cannot be obtained from direct measurements. Such responses may include the vibration amplitude of a newly developed seismic base isolation system undergoing extreme earthquake loading without building a full-scale physical model (Koh and Kelly 1990); or the performance characteristics of fuel-rod cladding in a nuclear reactor in the event of a natural disaster without having to undergo risky nuclear testing (Lassmann 1992). Also, these predictions often involve what-if scenarios that attempt to simulate future responses at untested settings, making the task of model validation even more difficult.

As a result, numerical models must be validated at settings where experiments are available to ensure that the predictions adequately represent a realistic, physical phenomenon at settings where experiments are unavailable. Traditionally, this validation task is handled solely focusing on the fidelity of the predictions to experiments through a process widely known as test-analysis correlation. Test-analysis correlation involves systematic comparisons of model simulations with experimental observations by establishing a quantitative validation metric (Doebling 2002, Oberkampf and Barone 2006). Typically, validation metrics are defined by a distance norm between model predictions and experimental observations.

The approach of solely focusing on fidelity however has proven to be problematic due to compensating effects from parametric uncertainties and model bias which can allow for multiple sets of input parameters to yield predictions with similar fidelity; a phenomenon known as non-uniqueness (Berman 1995). What is more, many of the assumptions made during initial development of the model regarding the formulation of

mathematical equations tend to have profound effects on the sensitivity of the model's predictions to uncertainties in the input parameters (Elishakoff 1995). If incorrect assumptions are made in the model formulation, slight variations in the input parameters can lead to drastic degradation in the model's predictive accuracy (Belegundu and Zhang 1992, XiaopingDu and WeiChen 2002, Au et al. 2003). The degree of sensitivity of a model's predictions to variations caused by uncertain input parameters, such as uncertain material properties or uncertain boundary conditions, is formally known as the model's robustness-to-uncertainty (Phadke 1989, Taguchi 1993, Du and Chen 2000, Hemez and Ben-Haim 2004). Based on this definition, a model that has a higher robustness-to-uncertainty will produce more consistent results even in the face of uncertain input.

With the increasing complexity of today's modern engineering challenges come gaps in knowledge of how to accurately simulate the complex behavior taking place. This lack of knowledge may manifest itself, for instance, as uncertainty in the model input parameters. If left unaccounted for, these input parameter uncertainties can have detrimental effects on the accuracy of model predictions, possibly leading to unforeseen catastrophic failures in engineered systems and threats to public well-being. Therefore, a thorough evaluation of these uncertainties and their effects on the model predictions are necessary.

This thesis presents a robust-satisficing approach for model evaluation that assesses the probability of success for satisficing the fidelity threshold for a given amount of uncertainty in the input parameters. This approach follows three distinct steps to evaluate the model's predictions. First, the fidelity of a given model form is evaluated at

various, predefined levels of threshold fidelity. Next, the uncertainty in the input parameters, represented as nested, unbounded intervals, is propagated through the model to evaluate the uncertainty in the predictions. Finally, by evaluating the probability of success of the model in satisficing the predefined threshold fidelity, a degree of confidence in the model form is quantified. These three steps ultimately lead to the evaluation of the model's prediction fidelity, robustness to uncertainty and probability of successfully satisficing the fidelity threshold as well as the trade-offs between all three attributes.

To summarize, this thesis advocates that trying to achieve a model which perfectly matches observational data, in the sense that traditional, fidelity-based model calibration is carried out, is infeasible due to unavoidable compensations between various forms of errors and uncertainties in model predictions and experiments. Therefore, this thesis asserts that one must evaluate a family of plausible models that satisfice a desired level of accuracy relative to the model's intended use. An advantage of this approach is that, in the face of severe uncertainty in parameter values, multiple alternative model forms that satisfice the same fidelity threshold can be further distinguished based on their probability of successfully satisficing that fidelity threshold. Furthermore, the trade-off between fidelity, robustness to uncertainty and probability of successfully satisficing the fidelity requirement is presented as a decision making tool.

1.2 Organization of the Thesis

This thesis begins by providing background knowledge of existing techniques for quantifying modeling uncertainties and, thus, for evaluating the predictive capabilities of numerical models. Chapter three then explains in detail the new approach for model evaluation presented in this thesis, henceforth referred to as probabilistic treatment of robust-satisficing approach. Chapter three demonstrates the application of this new approach on an academic example using three different model forms. Chapter four applies the probabilistic treatment of robust-satisficing approach to a case study of a structural portal frame with uncertainty in the model form as well as the input parameters for connection stiffness and demonstrates the viability of the method for identifying the most preferred model form. Chapter five is an extension of the case study presented in Chapter four in that the models are then further evaluated using a triple-objective optimization of fidelity, robustness, and probability of success, which implements the use of NSGA-II. Finally, Chapter six briefly summarizes the main contributions of the thesis, and then discusses the limitations of the new model evaluation method along with the future direction.

CHAPTER TWO

BACKGROUND

In the past half century, scientists and engineers have come to realize the growing need for assessing the level of uncertainty in model predictions (Elishakoff 1995). This has led to the development of numerous methods for analyzing models that attempt to simulate the physics of realistic phenomena. Uncertainty quantification methods available in the established literature that are relevant to this thesis include probabilistic methods, interval analysis methods, possibility theory, and methods employing nested convex sets. The following sections will give a brief description of each of these methods.

2.1 Probabilistic Methods

Perhaps the most extensively applied method is probabilistic analysis, where the central concept is to represent the uncertainty in the model input parameters using statistical distributions based on measurement data, published literature or experience. The probabilistic distribution is used to represent the parameter of interest, where the distributions assign probabilities to the possible values of the parameter, therefore acknowledging uncertainty in any single value. After characterizing the uncertainty in the model parameters, the second step in this method is to propagate the uncertainty through the model in order to determine the uncertainty's effect on the model's predictions. Typically, a probability distribution of prediction values is obtained.

The Monte Carlo method is widely used to carry out the forward propagation of uncertainty (Wu et al. 1990, Hills and Trucano 1999, Pepin et al. 2001). This method

involves executing a large number of simulations using random values of the input parameters generated by sampling their respective probability distributions, with the ultimate goal of creating a distribution of prediction values. According to the method, the prediction with the highest frequency of occurrence is the most likely prediction. However, because of the large number of simulations required for this method, Monte Carlo method can become infeasible, especially when the simulation model is more computationally demanding. Another very common technique is known as the Advanced Mean Value method, which employs a truncated Taylor's series expansion of the model form to evaluate the change in the model's predictions with changes in the input parameters (Wu et al. 1990). This method is generally suited for more time-costly computer analysis and is known for requiring less functional evaluations (Pepin et al. 2001).

2.2 Interval Analysis

Although the probabilistic techniques are well established and have accrued much success in past research, they require prior information about the probability distributions, and small errors in the distribution data can lead to large errors in the prediction distributions (Elishakoff 1995). Therefore, where probabilistic information about the properties of a system is not available, other non-probabilistic techniques may be better suited. One popular non-probabilistic technique is interval analysis, in which the uncertain parameters are expressed by a range of values (Rao and Berke, 1997). The information regarding the distribution of the parameters within that range need not be known, and therefore, there are infinite possible values of the uncertain parameter within

that range. The objective of interval analysis is then to discover upper and lower bounds of prediction values, which satisfice the equations that constitute the model form; or also put, the analysis finds the least favorable and most favorable predictions that still satisfice the set constraints (Qiu and Wang, 2003). Moens and Vandepitte (2005a) describe an approach to interval analysis that uses hypercube approximations to estimate the domain of the exact solution set. The main disadvantage to traditional interval analysis, however, is that the range of prediction values gives no consideration to the likelihood of a particular outcome.

2.3 Possibility Theory

Another popular theory for quantifying uncertainty, which can be seen as a combination of probability theory and interval analysis, is known as possibility theory. Possibility theory is seen as an alternative to probability theory in that it provides a measure that defines the degree to which an event can occur (Moens and Vandepitte 2005a). More specifically, this theory assigns a degree of possibility between 0 and 1, with 0 representing an impossible situation and 1 representing a common situation (but not guaranteed), to each element in a set of elements describing the validity of its description. The set of possibilities then defines a possibility distribution, which conveys the amount of existing knowledge about the values in the set (Dubois 2006). Possibility values are determined via a normalized mathematical function called the possibility function. The fundamentals of this theory are extended from the concept of fuzzy logic, which was first introduced by Zadeh (1965). Formally, fuzzy logic is centered on the capability of defining incomplete information through the use of fuzzy sets (Elton, Juang

and Lin 2000). To reiterate, these sets distinguish between elements of the set by varying degrees of membership using a membership function. This function assigns a normalized grade of membership to each element defining the level of certainty to its description. Furthermore, the membership range is subdivided into various levels, typically called α-levels, and where the value of the membership function, which defines the input uncertainties, intersects with each level defines an interval. Then an interval analysis is performed using the intervals just defined, resulting in corresponding intervals of results for each α-level (Moens and Vandepitte 2005b).

2.4 Convex Modeling

Convex modeling is another non-probabilistic theory that can be implemented for the quantification of uncertainty. The main idea of this approach that differentiates it from the previous theories mentioned is that convex modeling is an approach for bounding uncertainty. For instance, uncertain parameters can be bound to a certain value, or uncertain functions can be bound by an envelope of functions or by an integral. The objective is to find the lower and upper bounds of a model which are consistent with some given quantity of information (Ben-Haim 1994). This is contrary to previous theories that instead use mathematical functions defined over a domain of events. Here, an event refers to a set of physical parameters used in the formulation of a mathematical function (Ben-Haim 1994). Also, the initial set of values for the said physical parameters are herein known as the nominal parameter values and are typically chosen based on prior information if available or expert judgment. These nominal values also represent the geometric center of the convex model from which the size of the model structure is

measured. Elishakoff and Ben-Haim (1990) provide a theorem which proves that possible realizations of uncertain events have a tendency to cluster into convex sets. However, the existence of non-convex uncertain events is acknowledged, and is associated with the characteristics of the events.

The clustering property of uncertain events is what gave rise to the theory of uncertainty quantification through convex modeling (Elishakoff and Ben-Haim 1990). Ben-Haim (1996) uses the concept of convex modeling to pioneer Information-Gap Decision Theory, a widely accepted approach to making informed decisions under severe lack of information. In this theory, he applies structured convex and non-convex models to quantify uncertainties associated with decision making.

In convex modeling, each function within one of the convex sets is said to represent a possible realization of an uncertain event. According to the theory of convex modeling, the uncertain predictions will tend to congregate into sets that vary in size based on the amount of uncertainty in the model's parameter values (Ben-Haim 1996). An important advantage of this theory, like the interval analysis method, is that probabilistic information about the distributions of the uncertain parameters is not required. One only needs estimations of the range of values for the uncertain parameters in order to effectively carry out the method. It also shows that convex modeling focuses on the geometric representation of uncertain events. This allows uncertainty analysis to be guided by the size and location of its convex sets; however, the structure of the convex model is initially assumed and held constant throughout the analysis. This concept and its

intricate role in the present method will be further dissected in the following chapter on failure surfaces and their role in defining fidelity and robustness.

CHAPTER THREE

METHODOLOGY

The approach described herein is a method that evaluates a model's ability to realistically simulate physical observations by quantifying the model's probability of successfully satisficing a given fidelity threshold value. In this chapter, the ability to discriminate between multiple models that yield similar fidelity predictions based on the robustness of these models to yield said fidelity under uncertainty is thoroughly discussed. This new approach is then demonstrated on a notional, proof-of-concept application. The method is comprised of three main steps: (1) defining a failure surface in parameter space (i.e., two uncertain parameters would yield a two-dimensional, plane failure surface, and three uncertain parameters would yield a volumetric failure surface) that quantifies the fidelity of the model output to physical observations; (2) exploiting the spatial variability of the failure surface to assess model robustness using increasing, unbounded sets of parameter values; (3) calculating the model's probability of successfully satisficing the fidelity requirement given increasing uncertainty in the input parameter values.

3.1 Defining the Failure Surface for Model Fidelity

The probabilistic treatment of the robust-satisficing approach relies on the assumption that all possible realizations of uncertain quantities which are consistent with some given amount of information will cluster together (Ben-Haim 1994). In this thesis, the uncertain quantities will be defined as uncertainty in the values of the model's input

parameters. Since each convex set of output is associated with some given quantity of information regarding the input, and the size of these sets depends on this available information, the change in the size of the set of uncertain realizations can be said to be directly correlated with the change in the information. Given this association, and the notion that all values contained within a convex set give prediction fidelity relative to experimental measurements no worse than that assigned to the set, a connection can be made between the values that are outside of the set bounds and failure to achieve that set's level of fidelity. Therefore, the concept of a failure surface will herein be defined as a geometric set of uncertain function realizations which all yield predictions with the same level of error from the experiments (i.e., fidelity to experiments).

Another bi-product of the mathematical simplification of a real physical system is that there may exist multiple model forms, which the modeler will have to choose from. This means that the modeler must decide which model is most appropriate for simulation of the phenomena of interest. This thesis advocates that in this selection importance should also be given to the robustness of a model. In other words, if two models display the same fidelity, the model that is more robust should be chosen for simulation. In convex modeling, given the same fidelity threshold, a larger geometric set of solutions translates to a more robust design compared to a smaller set (Ben-Haim 1995).

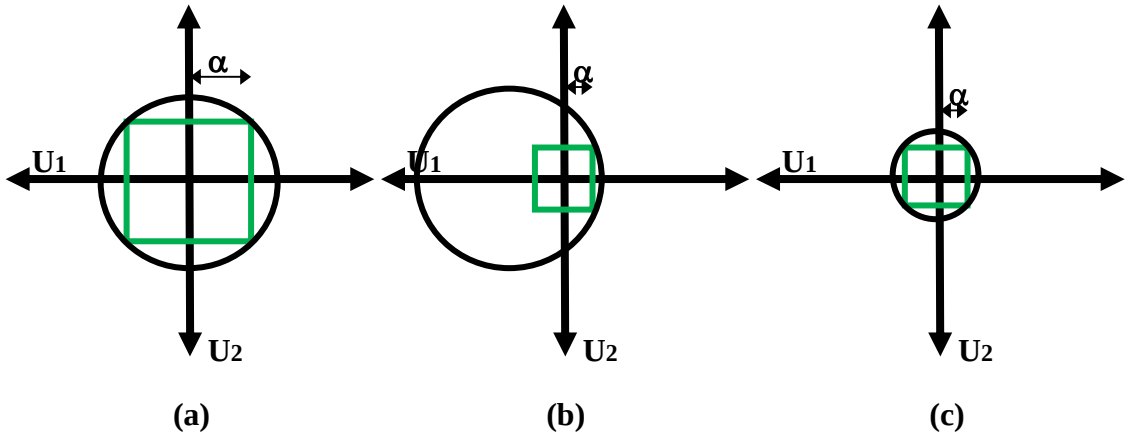

Figure 3.1: Failure surfaces for three different notional model forms (a) failure surface centered at the nominal parameter values (b) failure surface centered away from the nominal parameter values (c) failure surface centered at the nominal parameter values, yet fewer solutions

Figure 3.1 illustrates the concept of a model's failure surface for a given fidelity threshold value for a hypothetical model with two input parameters. In this figure, the abscissa and ordinate axes represent the uncertain input parameter values U1 and U2, respectively. Failure surface here is defined as the area encompassed by the geometric set (in this example a circle) representing all pairs of input parameter values that yield model output that is consistent with a specific fidelity threshold value. For instance, for each of the three models shown in Figure 3.1, there is an associated domain of acceptable parameter value pairs, which would guarantee a predefined level of fidelity to experiments. A contour drawn to envelope these acceptable parameter values would yield what is henceforth referred to as failure surface.

Hemez and Ben-Haim (2004) describe this phenomenon as *ambiguity*, which occurs when variables, such as input parameters or model forms, can interact to reproduce the data in more than one way. The α values shown in Figure 3.1 are a measure from the nominal parameter values of the model to the boundary of the failure surface. This is a common robustness measure associated with convex models of uncertainty called worst-case robustness analysis (Parkinson et al. 1993, Chen et al. 1996, Su and Renaud 1997, Lee and Park 2001, Au et al. 2003). Worst-case robustness analysis may use an expansion parameter, such as α in Figure 3.1, to quantify the level of uncertainty in the model output given uncertain input. It does so by expanding the size of the uncertain input domain until failure occurs (i.e., the expansion parameter reaches the boundary of the failure surface), hence the name worst-case analysis (Figure 3.2). In this sense, the model design is said to be totally immune to unexpected input variations that fall within the predefined intervals.

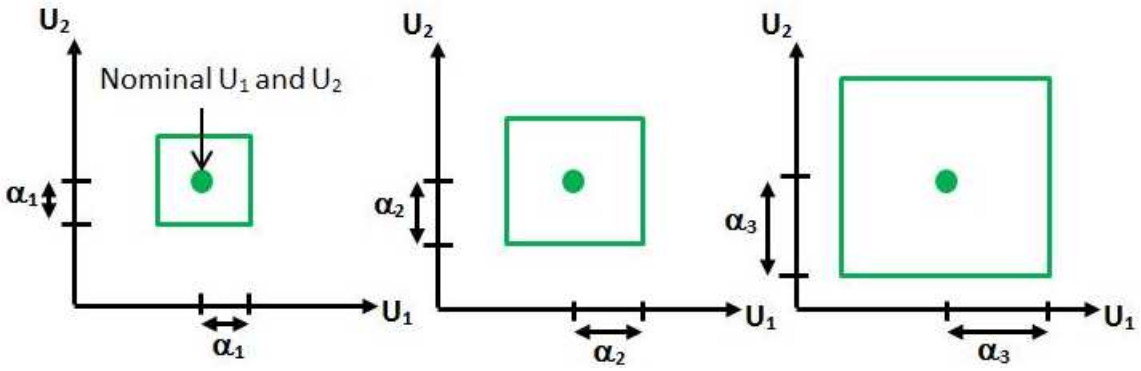

Figure 3.2: Demonstration of the expansion parameter α if the convex model was assumed to be uniformly bound

Worst-case robustness analysis is known to be conservative and can result in over-designing of the system being modeled (Mulvey, Vanderbei and Zenios 1995). Furthermore, this approach may create the problem illustrated in Figure 3.1. Figure 3.1(a) shows a model's failure surface that is centered at the nominal parameter values and displays a large domain of acceptable parameter values. Figure 3.1(b), however, shows a failure surface with the same parameter domain size as Figure 3.1(a), yet the surface is not centered at the nominal parameter values, and thus α stops expanding much earlier than it did with the model in Figure 3.1(a). On the other hand, there may exist multiple model forms where their domain of acceptable input parameter values are centered at the same values yet their domain sizes vary for the same fidelity value, as shown in Figure 3.1(c). Here, the failure surface may be centered at the nominal input parameter values but the model can only tolerate small deviations from those the nominal values before failing to satisfice the fidelity threshold. With the worst-case robustness analysis, the robustness of parts (b) and (c) would be quantified as equal for a given fidelity threshold. However, if the domain size was selected as the robustness measure, then the two models shown in (b) and (c) would be identified to have different robustness. As seen, neither approach is able to distinguish between these three models. Herein, the challenge arises to differentiate between these model forms as to determine which one will yield the most robust results considering their probability of successfully yielding the results with a minimum level of fidelity.

3.2 Derivation of the Failure Surface

As discussed in the previous section, this probabilistic treatment of the robust-satisficing approach presented herein relies heavily on the use of a geometric delineation of input parameter values that defines the varying levels of a model's fidelity, referred to herein as the failure surface. The term failure surface, in this thesis, stems from the concept of convex modeling of uncertainty in which all uncertain parameter values that lay on or within the boundary of the surface yield output within the *same* fidelity threshold value.

Let's consider a model M with n uncertain input parameters, $U_i, (i = 1,2, \dots, n)$, defining an n-dimensional parameter space, where

$$y_p = M(x, U_i, q) \quad \text{for } i = 1,2, \dots, n \qquad \text{(Equation 1)}$$

In this equation, y_p is the model output and x, U_i and q are the model input parameters. The x parameters represent a subset of the input parameters called the control parameters, which are known to the analyst and can be controlled during the experiment. These variables define the domain of applicability. The uncertain parameters U_i cannot be controlled by the analyst, yet they exhibit significant influence on the results of the model. The q variables represent all other variables in the model which are neither controlled nor uncertain.

Here, the analyst is assumed to have prior knowledge regarding the nominal (i.e. best estimate) values for U_i; however, their precise values or distributions are unknown. The fidelity of this model to reproduce reality with various input parameter values can be determined by exploiting the availability of experiments. For instance, fidelity can be

defined as the normalized deviation of model predictions from experimental measurements as given in Equation1:

$$R = \frac{\|y_o - y_p\|}{y_o} \qquad \text{(Equation 2)}$$

where R represents the norm of the error between the model predictions y_p and the experimental measurement y_o. In Equation 1, $\|\cdot\|$ indicates a suitable norm, such as a Euclidian distance, i.e. absolute geometric distance between two points; Mahalanobis distance, i.e. weighted distance between a point and a population that considers the correlations; Bhattacharyya distance, i.e. weighted distance between two populations that also considers the correlations.

Assuming that a n -dimensional parameter space contains a solution that can identically reproduce the results of an experimental measurement; i.e., $R_t = 0$, where R_t represents the predefined fidelity threshold, there would exist a single (unique) solution set of n model input parameters U_i that satisfice this requirement. If such a solution does not exist, then there will be a single (unique) solution that would yield the best fidelity (i.e., lowest R value) to experiments. Such unique, so-called 'best fidelity' solutions cannot be trusted however, due to the inevitable compensations between various forms of uncertainties and errors in the model. The problem is further compounded by the inevitable uncertainties in the experimental measurements y_o. All things considered, fidelity alone is an unrealistic indicator of a model's predictive ability.

Let's evaluate the functional form of Equation 2 for a model with a two-dimensional parameter domain U_i corresponding to the input parameters U_1 and U_2 given by the following generalized model:

$$R = f(U_i) \qquad \text{(Equation 3)}$$

where R represents the fidelity metric, or level of disagreement between the model predictions and experimental observations, to be minimized. This representative functional form of Equation 3 is illustrated in Figure 3.3.

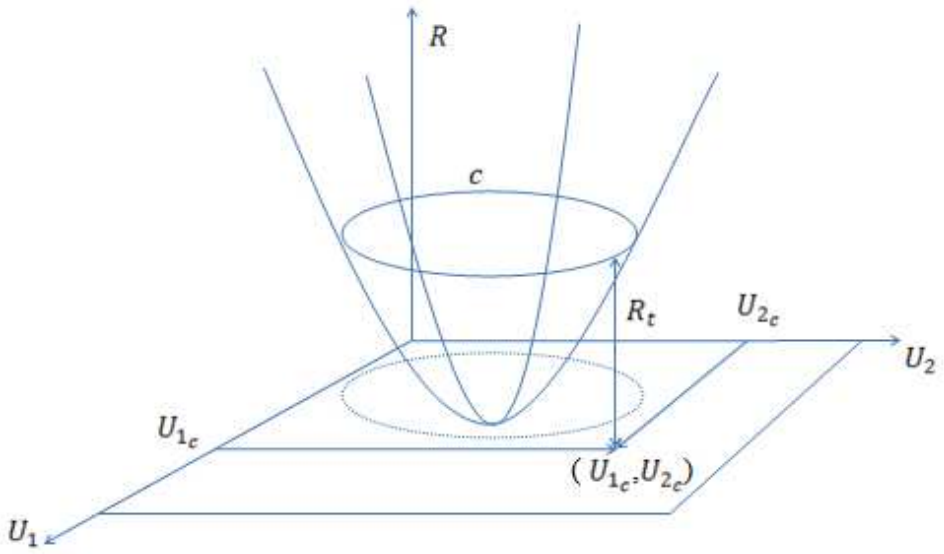

Figure 3.3: Depiction of a minimization function in two-dimensional parameter space

The goal is to find all coordinate pairs of U_1 and U_2 in this three dimensional domain that give '*the same*' values of R_t (within acceptable tolerance limits). Thus, the analyst desires the coordinates of points in the U_1- U_2 plane that satisfice the following conditions:

$$f(U_{1_c}, U_{2_c}) = R_t \qquad \text{(Equation 4)}$$

where R_t is the desired fidelity threshold of our model predictions. Equation 3 can be reorganized into the following form:

$$f(U_{1_c}, U_{2_c}) - R_t = 0 \qquad \text{(Equation 5)}$$

Based on Equation 3, it is clear that for any other point that is not on our desired failure surface we will have the following condition:

$$(U_1, U_2) \notin c \rightarrow f(U_1, U_2) - \mathrm{R}_t \neq 0 \qquad \text{(Equation 6)}$$

where c represents the domain of parameter values that are bounded by the failure surface at the fidelity threshold R_t. Therefore, by defining an objective function in the following form and minimizing the z value, the points on the failure surface can be found.

$$z = |f(U_1, U_2) - R_t| \qquad \text{(Equation 7)}$$

where z is the tolerance limit, i.e. absolute value of the discrepancy between the prediction fidelity and the predefined fidelity threshold. However, a tradeoff exists between the solution accuracy of z and the time to solution. In other words, the smaller the value of z, the longer the computation time.

The objective function for minimization can now be formatted into the following general equation:

$$\min z = \min|f(U_1, U_2) - \mathrm{R}_t| \leq 10^{-7} \qquad \text{(Equation 8)}$$

In Equation 8, the threshold value of z was decided to be 10^{-7}, but it should be noted that this value is subjective and case specific.

Most optimization approaches require an initial, starting point for the algorithm. The initial starting point used in this method is the nominal values of the uncertain input parameters. The second point is then chosen randomly within a specified allowable range. This range will also be based upon the analyst's judgment. Each point after is selected as the calculated average of the two previous points. However, if a selected point does not

satisfice the condition given by Equation 6, the algorithm starts over from the initial point. This iterative process continues until the desired number of points j that satisfice Equation 8 are found. The collection of these points for a single fidelity threshold value makes up the failure surface. This algorithm can be implemented to generate multiple failure surfaces for a single model, each corresponding to a specific fidelity threshold value. A flow chart describing the algorithm's step-wise process is shown in Figure 3.4.

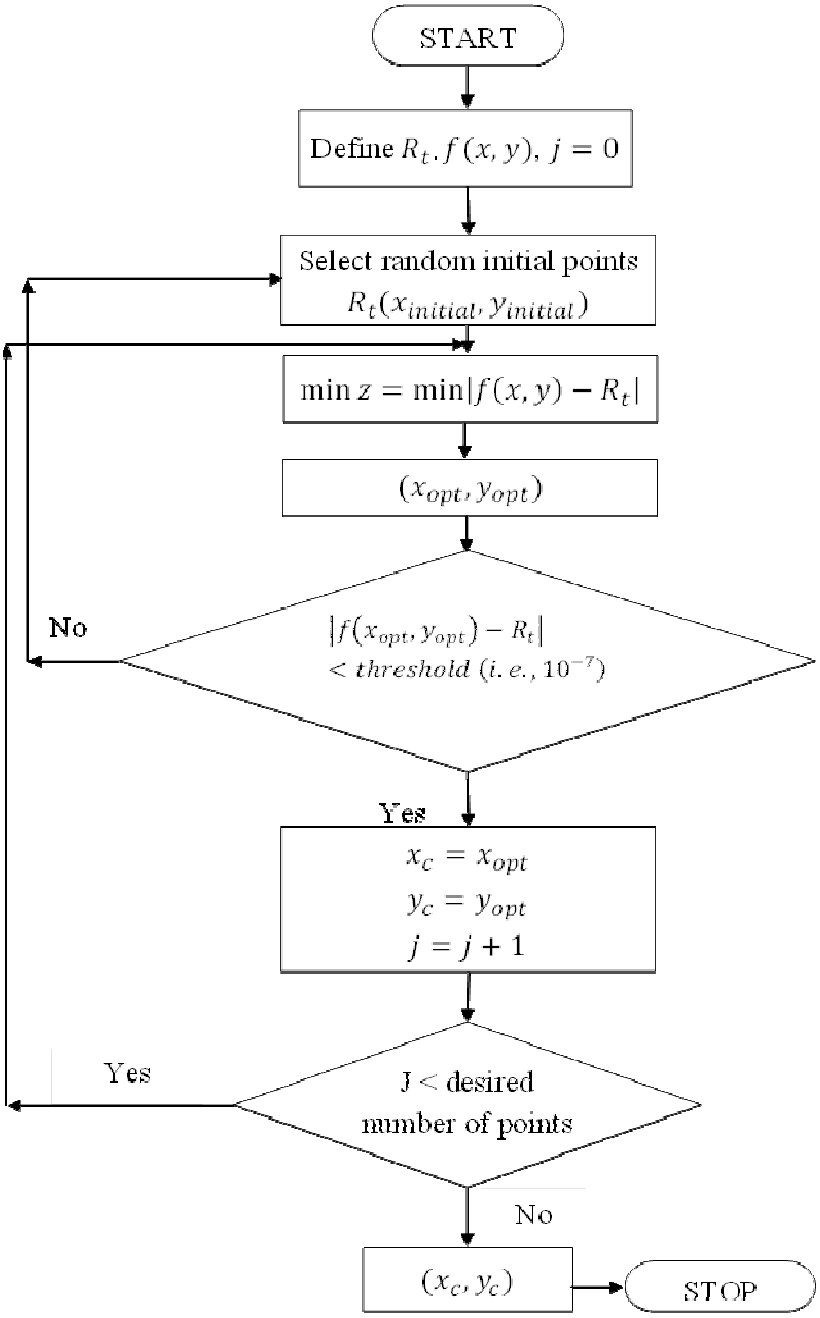

Figure 3.4: Flowchart of optimization algorithm used to define the failure surface of a two-dimensional uncertain parameter domain

To solve this minimization problem, a variety optimization methods can be implemented such as gradient-based minimization approaches (i.e., Newton's method, Steepest Descent Approach, Golden Section, fminsearch) or stochastic optimizations (i.e., Genetic Algorithms, Ant Colony Optimization, Cultural Optimization, Particle Swarm Optimization).

Naturally, the input parameter values associated with equivalent prediction fidelity can be linked together to form an individual failure surface as shown in Figure 3.5 for a two-dimensional parameter domain. Equation 8 provides the link between the input parameter values and the threshold fidelity. However, the value of fidelity threshold R_t need not be known initially since the current method evaluates the model for increasing levels of R so that the analyst can visualize how the simulation is behaving as more uncertainty is introduced into the input parameters. This evaluation therefore naturally leads to a trade-off analysis, which is discussed later in this chapter.

$$\{U_i : \frac{\|y_o - y_p\|}{y_o} \approx R_t \qquad i = 1,2,\dots,n\} \qquad \text{(Equation 9)}$$

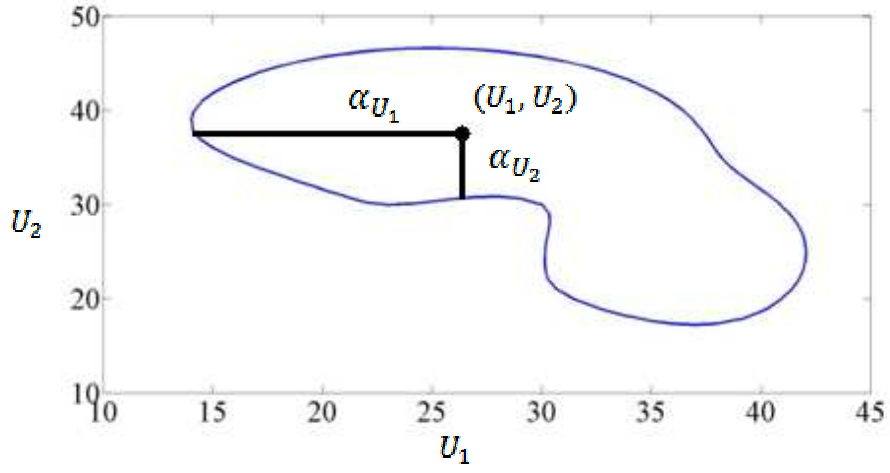

Figure 3.5: Example failure surface for a single level of fidelity

From Figure 3.5, it can be seen that the failure surface may not assume a specific geometric shape, such as a circle, square or ellipsoid. Moreover, the allowable ranges for parameter values that satisfice a given fidelity requirement may assume different values in different parameter dimensions as shown by α_{U_1} and α_{U_2} in Figure 3.5. Thus, assessing the entire failure surface allows for a complete evaluation of the amount of uncertainty that can be tolerated in the model input parameters and still satisfice a given fidelity requirement.

The amount of uncertainty that can be tolerated, which can be defined through the use of a variety of metrics, yields an indication of the *robustness* of the model predictions to uncertainty. For instance, Ben Haim (1996) defines robustness as the maximum allowable deviation from the nominal value in one of the input parameter dimensions in which failure cannot occur as illustrated in Figure 3.6. The symbol α shown in Figure 3.6 is a metric used in convex modeling of uncertainty to measure the amount of uncertainty that is consistent with 100% success of a system's operation (Ben-Haim 1996). The magnitude of α grows with each increase in the allowable uncertainty in the system (i.e., increase in the size of the failure surface in Figure 3.5). Therefore, in regards to the geometry of convex sets, α is also known as the uncertainty parameter, and is used to evaluate the amount of acceptable uncertainty a system will tolerate before failure occurs. Although a circle is shown in Figure 3.6, based on the information available to the modeler regarding the uncertainty within the model, a number of geometrical configurations can be used to represent the uncertainty (Ben-Haim 2006). For instance,

ellipsoidal models are a frequent configuration encountered in convex models of uncertainty.

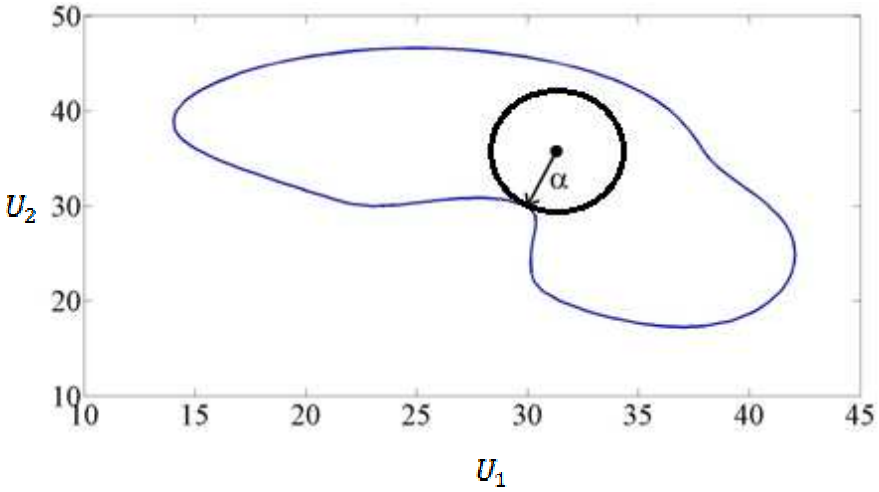

Figure 3.6: Illustration of the uncertainty parameter α as implemented in worst-case robustness analysis methods

There are other alternative definitions for robustness depending on the characteristics of the problem; for instance, Hample (1971) qualitatively defines a robust parametric model as one whose distributions of the parameter estimations are defined by weak-continuous functionals. Taguchi (1993) originally defined robust design as the ability to minimize the effects of the causes of variations without eliminating the causes. Taguchi's method has been widely accepted as a standard for the quality control of industrial designs (Phadke 1989; Chen et al. 1998). Regardless of the metric used to define robustness, it can be said that the size of the failure surface in Figures 3.5 and 3.6 is indicative of the robustness of the model against uncertainty.

Of course, as the fidelity threshold is increased, the uncertainty that is allowed in the input parameters naturally increases as a larger number of parameter sets can satisfice this increasingly less stringent fidelity requirement. If the process is carried out for multiple levels of fidelity threshold, a hyper-dimensional volume can be obtained. One such volume is illustrated in Figure 3.7 for the two-dimensional domain shown earlier in Figures 3.5 and 3.6. From here, the decision maker can evaluate the trade-off between fidelity, robustness-to-uncertainty and probability of success and make an informed decision in determining the appropriate fidelity requirement for the model.

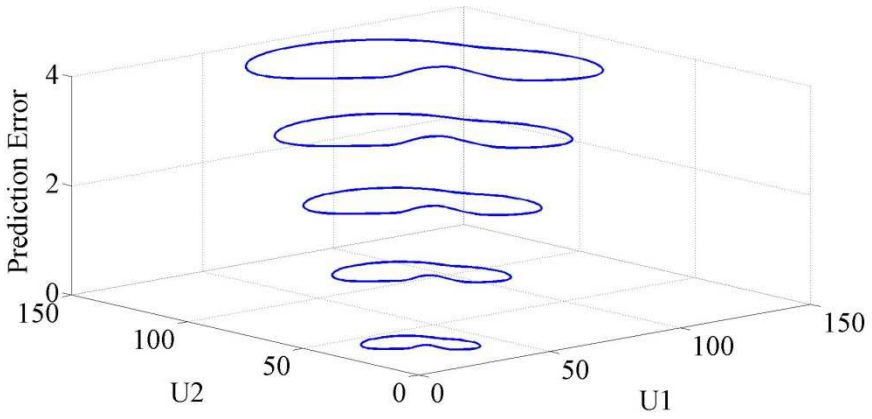

Figure 3.7: The domain of parameter values (U_1 and U_2) increasing with increasing error in the predictions (i.e., decreasing fidelity) of an example model

Figure 3.7 also demonstrates the relationship between the size of the failure surface and the fidelity (i.e., prediction error). Here, a larger failure surfaces entails more solutions or acceptable pairs of input parameter values that will satisfice the fidelity threshold. Furthermore, Figure 3.7 visually demonstrates the paradigm proposed by Ben-Haim and Hemez (2011), in which the relationship between fidelity and robustness-to-

uncertainty are mutually antagonistic. In other words, one cannot improve one aspect without deteriorating the other. Therefore, when selecting a simulation model that will best represent the physical system in question, a model which yields high fidelity predictions is likely to lack robustness, and if left unchecked, can lead to low fidelity predictions when slight variations are introduced into the modeling parameters. This confirms the necessity to base the process of model selection on more than just prediction fidelity, but also on the effect of uncertainty on the fidelity.

Also note that in Figure 3.7, the rate at which the size of the failure surfaces are growing indicates the compromise between the fidelity threshold and robustness against uncertainty for a given model, a quality of the convex modeling, robust-satisficing approach that was established by Ben-Haim (1996). If the model displays significant gains in robustness with only slight loss of fidelity, it could be considered a favorable trade-off in the eyes of the model developer, since this would mean that the simulation model has gained immunity to the parameter uncertainty while still producing accurate predictions. On the other hand, if it is shown that the model's fidelity degrades quickly with little gain in robustness, this could mean that there exist significant inconsistencies in the model. Herein lies the basis of this presented method as a decision-making tool for model developers.

3.3 Probabilistic Evaluation of Satisficing the Fidelity Threshold

With the failure surface defined, the robustness of the model to the uncertainty in the input parameter values can be quantified via probabilistic assessment of the model's ability to satisfice the fidelity threshold. This is necessary since it is the model's

predictions that are compared to the observed data, and there needs to be a link between the amount of uncertainty in the system and model's ability to produce robust predictions. This defines the core of the novel probabilistic treatment of robust-satisficing approach.

While worst-case robustness analysis does not allow for any failure to occur, in the proposed method, the robustness metric is defined as the measure of the allowable deviations from the nominal model input parameters for a given probability of successfully satisficing a fidelity threshold requirement. Evaluating a model's *probability of successfully satisficing a fidelity threshold* invokes the concept that there is an "acceptable" tolerance for failure of said threshold.

By exploiting the failure surface that was derived in Section 3.2, the robustness evaluation can be carried out by assessing the spatial variability of the input parameters within the domain defined by the input parameters. Hence, given prior knowledge regarding the best estimate (i.e., nominal) values for the input parameters, the failure surface for a given model can be used to define that model's probability of successfully recreating the phenomenon being simulated. This can be accomplished by defining nested sets of the input parameters around the nominal values. The phrase "nested sets" refers to monotonically increasing the size of each set, or also put, the domain of the previous set is always contained in the domain of the successive set.

The use of nested sets implies that the bounds of input parameter values are sequentially increased to sample a sufficiently large domain of values so that all feasible values of the input parameters are attempted. Ultimately, model robustness is evaluated by comparing the parameter values contained in the failure surface with the increasing

sets of input parameter values that are centered around the nominal parameter values. The ratio of the number of input parameter solutions within the failure surface that match the input parameter values within the nested sets to the total number of values sampled in the nested set is used to determine the probability of successfully satisficing the threshold fidelity requirement. The sets of parameter values need to be sampled thoroughly to achieve an accurate determination of probability of successfully satisficing the fidelity requirement. This approach for evaluating fidelity and robustness results in a much more computationally efficient technique than traditional Monte Carlo techniques.

3.4 Proof of Concept Demonstration

3.4.1 Robustness Evaluation

A proof-of-concept demonstration of the aforementioned procedure was carried out on three mathematical models. In this academic example, these three model forms are assumed to be developed to simulate the same phenomenon. All three models share the ability to satisfy the same fidelity thresholds with non-unique sets of input parameter values. The challenge herein is distinguishing which model form best represents the phenomenon being simulated.

First, let's consider a model whose failure surface centered at the nominal parameter values. This is depicted as Model 1 in Figure 3.8. This figure shows that by expanding the uncertainty parameter α the probability of the model being able to successfully satisfy the associated fidelity threshold deteriorates. This is representative of increasing the uncertainty in the input parameter values. Here, the approximately 14% increase in α between Figure 3.8(a) and 3.8(b) leads to a 20% decrease in the model's

probability of satisfying the fidelity requirement, and the 12.5% increase in α from Figure 3.8(b) to 3.8(c) leads to a 17% decrease in the probability of success. It should also be noted that the α increase for U_1 and U_2 does not need to be the same.

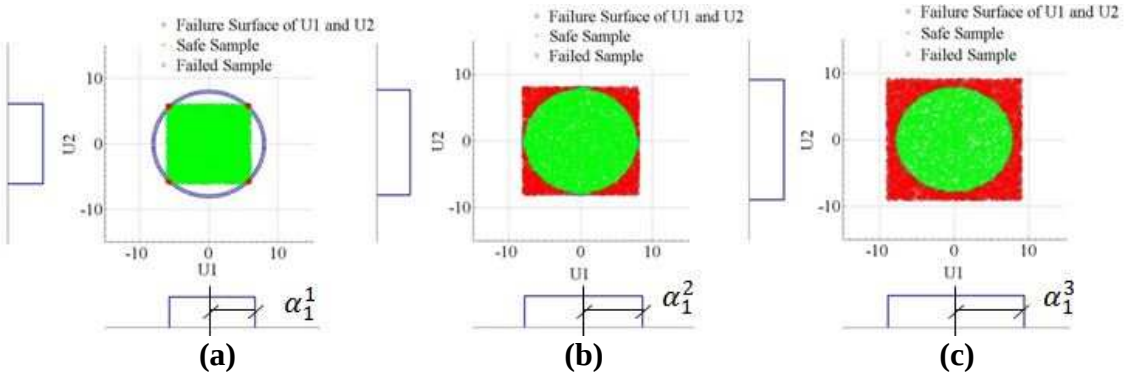

Figure 3.8: Sampling of Model 1 for three interval ranges given equal fidelity thresholds (a) Probability of Success = 99%; (b) Probability of Success = 79%; (c) Probability of Success = 62%

Let's now consider a model whose failure surface is not centered at the nominal parameter values, henceforth referred to as Model 2 (Figure 3.9). Figure 3.9 depicts the results of the sampling procedure on Model 2 for the same fidelity threshold value as that used for Model 1 in Figure 3.8.

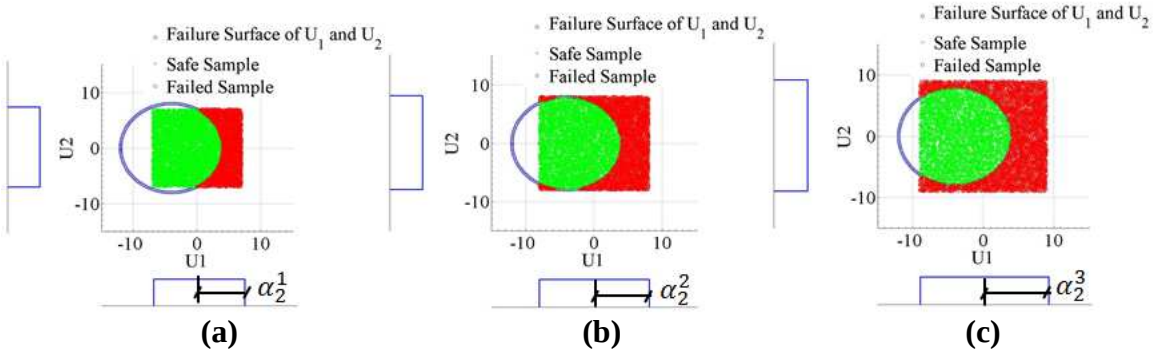

(a) **(b)** **(c)**

Figure 3.9: Sampling of Model 2 for three interval ranges given equal fidelity thresholds (a) Probability of Success = 70%; (b) Probability of Success = 62%; (c) Probability of Success = 54%

Now consider a third model, henceforth referred to as Model 3, that is centered at the nominal parameter values like Model 1; however, the failure surface is much smaller. Figure 3.10 illustrates how the proposed method discriminates between the robustness of models that otherwise would be considered similar according to the worst-case robustness analysis approach described in Chapter 2 of this thesis. This figure shows the comparison between Model 2 and 3 using the proposed method for the same fidelity threshold value as well as the same magnitude of the uncertainty parameter α. If the robustness analysis was based solely on the worst-case approach (i.e., the largest α value reached before breaching the failure surface) then Models 2 and 3 would be described as having similar robustness since the distance from the nominal values to the failure surface is the same for both models. However, given their failure surfaces in Figure 3.7, one can see that Model 2 has a much larger domain of parameter values that satisfy the fidelity requirement, although Model 2 has a failure surface that is centered on the

nominal parameter values. Based on the proposed method, Model 2 has a 54% probability of successfully satisfying the fidelity requirement, while Model 3 has a 15.5% probability of satisfying the fidelity requirement. Thus, the proposed method successfully distinguishes between the predictive capabilities of the two models. The following section will discuss how to analyze each model's ability to handle the increasing uncertainty as well as define a metric that will distinguish each model based on their immunity to the uncertainty.

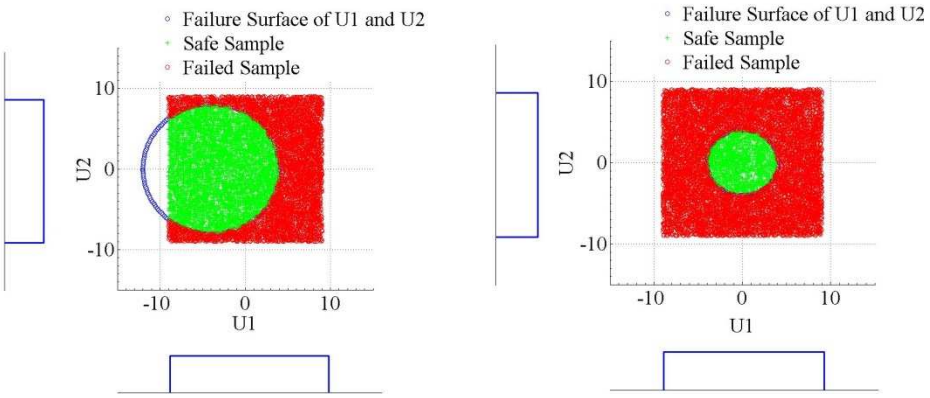

(a) **(b)**

Figure 3.10: Comparison of Probability of Success for (a) Model 2 to (b) Model 3 for equal fidelity threshold requirement and parameter sample interval

3.4.2 Trade-off between Robustness to Uncertainty and Fidelity-to-data for a given Probability of Success

In general, a model is considered validated when it can be said with confidence that the formulation of the model is representative of the physical system throughout the entire domain of applicability (Hemez and Ben-Haim 2004). Therefore, it is necessary to analyze a model over all plausible values of the uncertain input parameters. Of course,

the extent of plausible parameter values is based solely on the amount of knowledge available about the parameter values. This is yet another decision to be made by the analyst. This evaluation then illustrates how each model is affected by the increasing uncertainty over all plausible values of the uncertain input parameters.

Here, the approach uses unbounded, monotonically increasing sets of the input parameters represented by the uncertainty parameter α centered at the nominal parameter values to compare spatially within the parameter domain contained by the failure surface. Since this method focuses on quantifying robustness based on the clustering of possible events that are consistent with a given level of information and not on ranking the frequency or possibility of occurrence, less prior information is necessary for analysis. This is a critical advantage to the proposed method that has also been emphasized by Ben-Haim (2006).

This process must then be carried out for increasing levels of fidelity (i.e., increasing sizes of the failure surfaces) as well as the increasing uncertainty in the input parameters just previously discussed. Then the trade-off relationships between fidelity, uncertainty parameter, and probability of successfully satisfying a defined fidelity threshold should be analyzed to determine the most preferable model (i.e., displaying favorable robustness and fidelity attributes simultaneously). This procedure was carried out for the three academic models shown earlier in Figures 3.8, 3.9 and 3.10 and the results are given in Figures 3.11, 3.12 and 3.13 for comparison of these three different model forms.

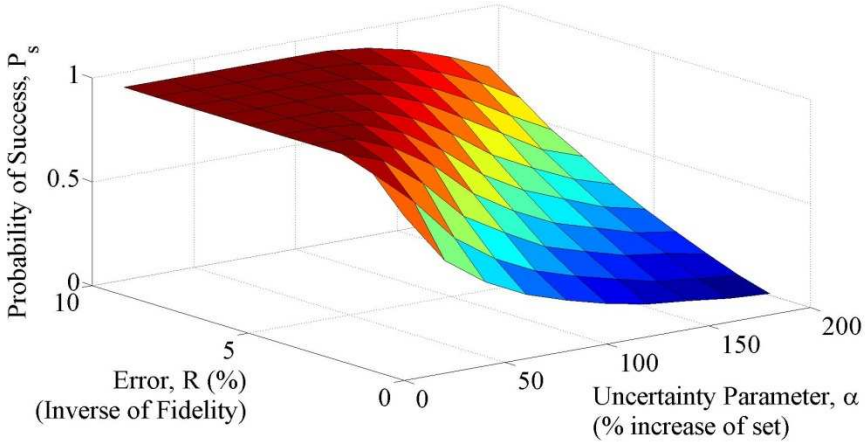

Figure 3.11: Trade-off between Robustness to Uncertainty and Fidelity-to-data for a given Probability of Success for Model 1 (refer to Figure 3.8)

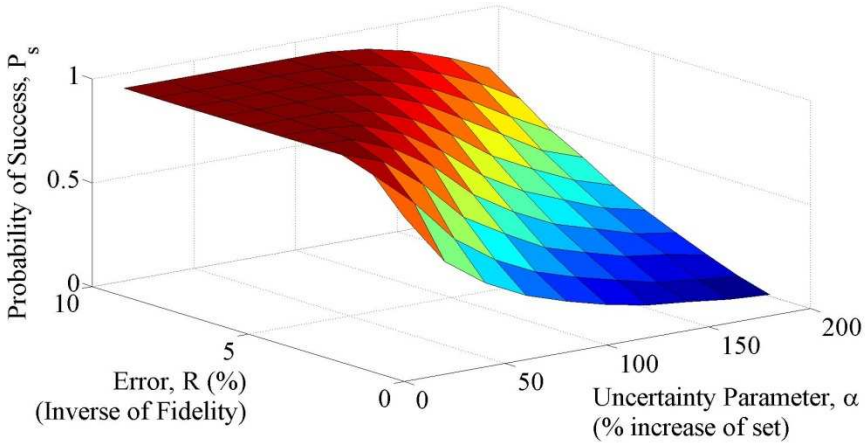

Figure 3.12: Trade-off between Robustness to Uncertainty and Fidelity-to-data for a given Probability of Success for Model 2 (refer to Figure 3.9)

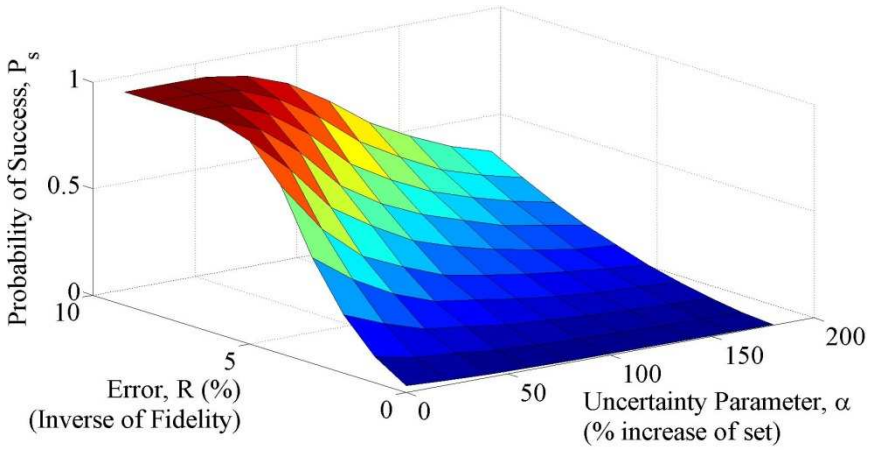

Figure 3.13: Trade-off between Robustness to Uncertainty and Fidelity-to-data for a given Probability of Success for Model 3 (refer to Figure 3.10)

In Figures 3.11, 3.12 and 3.13, one can visualize how all three attributes (i.e. fidelity, robustness of the said fidelity and probability of satisfying the fidelity) of this method interact for these three different models. Although the numerical results differ between all three models, the trends follow the same pattern. As the uncertainty parameter α increases, the probability of successfully satisfying the fidelity requirements deteriorates as expected. The opposite trend occurs for the error in the model predictions. It should be noted that fidelity has an inverse relationship to prediction error (i.e., high prediction error means low fidelity and vice versa). In all three models, as the error is allowed to increase, there exists more possible values of the input parameters that can satisfy the fidelity requirement, and therefore the probability of success increases. However, by observation of Figures 3.11, 3.12 and 3.13 it appears that Model 1 has the most favorable reaction to the increasing uncertainty parameter.

There are three scenarios that exist for the decision maker (DM) in this process. First, the DM can choose a probability of success that he or she feels establishes a reliable level of confidence in the model, and then assess the trade-off between fidelity and the uncertainty parameter. Another scenario would be to establish a fidelity requirement up front, then analyze the results for probability of success versus the uncertainty parameter. Here, the DM would be able to assess a model's prediction ability based on how their probabilities of successfully satisfying the fidelity requirement change with the increasing uncertainty parameter. The third scenario would be to initially establish a certain magnitude of the uncertainty parameter α and then analyze the change in probability of success with the change in the fidelity requirement. A specific fidelity threshold can be decided upon based on analysis of how the fidelity varies given an increasing uncertainty parameter. Once this predefined level is reached, the system is deemed to be robust to the level of uncertainty (value of the uncertainty parameter) that corresponds to that fidelity threshold (i.e., will yield predictions accurate to within the fidelity threshold with a given probability of success).

The robust-satisfying approach taken is then defined as the highest magnitude of the uncertainty parameter that a model can achieve for a given probability of successfully satisfying a fidelity threshold requirement. In other words, given several model forms using the same uncertain parameters, the model with the largest uncertainty parameter evaluated at the same probability of success is the most robust. This concept can be formulated mathematically as follows:

$$\hat{\alpha} = max\{\alpha: (R(\alpha) \leq R_t * P_s \geq P_{s_t})\} \qquad \text{(Equation 10)}$$

where $\hat{\alpha}$ represents the maximum robustness of the model's predictions, P_s represents the probability of successfully satisfying the fidelity threshold, P_{s_t} is the probability of success threshold, $R(\alpha)$ is the fidelity associated with a given uncertainty parameter requirement, and R_t is the threshold fidelity value. This concept is also illustrated in Figure 3.14 for a constant magnitude of the uncertainty parameter α.

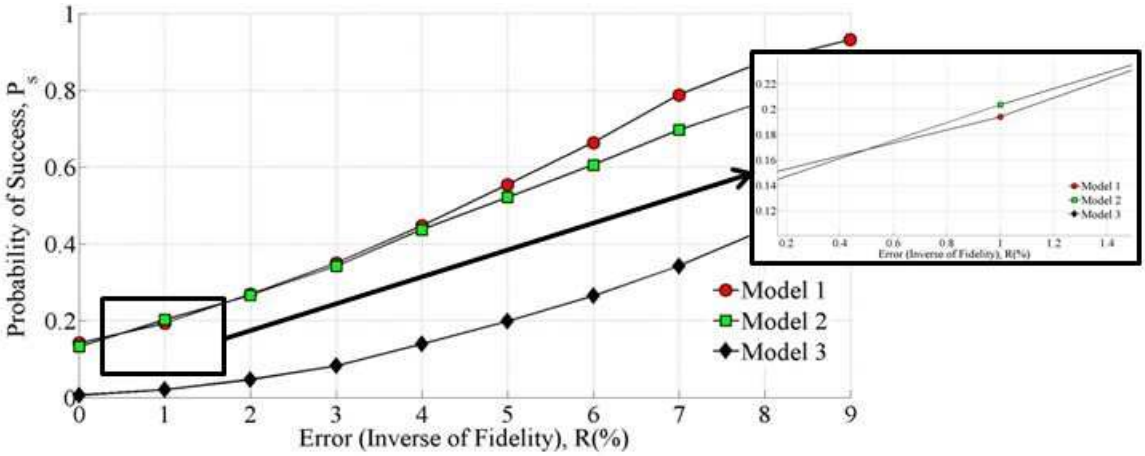

Figure 3.14: Probability of success versus prediction error for a constant α

Figure 3.14 also illustrates a unique phenomenon in this decision making process known as preference reversal. For Models 1 and 2 in Figure 3.14, between 0 and 2 percent error, the two models can be seen exchanging roles as the more successful model, as shown by the enlarged window. At approximately 0.5% error Model 2 yields a higher probability of success than Model 1, yet this outcome reverses at 2% error and continues this trend. This concept, referred to as *preference reversal*, shows that a model may seemingly produce accurate predictions for a certain phenomenon; however the

underlying uncertainties inherent with the model formulation can cause fluctuating behavior that another model may more suitably manage.

CHAPTER FOUR

CASE STUDY APPLICATION: STEEL MOMENT RESISTING FRAME WITH UNCERTAIN CONNECTION STIFFNESS

The proposed procedure developed in this manuscript is demonstrated on a case study of a two-story, two-bay, steel portal frame shown in Figure 4.1. In steel frame structures, connection stiffness values are typically highly uncertain due to natural variability in material properties, geometry and construction practices. These parameters are typically calibrated against experiments in an attempt to converge on their true values and, thus, in this study are treated as calibration parameters, K_1 and K_2. In this case study, aside from being also unaware of the exact values of K_1 and K_2, the model developer is also assumed to have an inaccurate knowledge of the underlying shear deformation behavior of the system. . As a result, multiple model forms with varying accuracy of shear deformation representation and with uncertain input parameters are developed.

The model developers are assumed to have experimental evidence to calibrate the uncertain parameters of the model. Accordingly, synthetic experimental data are generated in the form of displacement responses of the frame using an exact model that accurately accounts for the effects of shear deformations and also uses the assumed exact values of K_1 and K_2. The goal of these experiments is to determine which model best represents the experiments given uncertain input parameters.

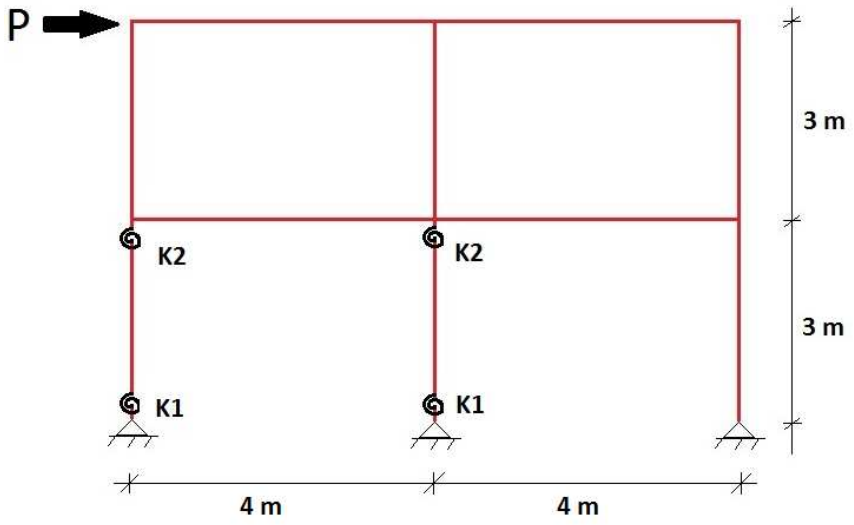

Figure 4.1: Two-bay, two-story portal frame with rotational springs at the top and bottom of the first story left and center columns

Aside from uncertainties in connection parameters, uncertainties also exist within the model due to assumptions and simplifications made to the governing equations, widely known as model form error (Draper 1995, Kennedy and O'Hagan 2001, Atamturktur et al. 2012, Farajpour and Atamturktur 2012). Furthermore, these assumptions and simplifications can allow for multiple model forms to yield similar results, drawing into question which model form is most representative of the real phenomenon.

Recognizing that no model is perfect, the model developer herein is assumed to be unaware of the accuracy of which the shear deformations are accounted for. Thus, besides the model that is used to generate the synthetic experiments, two inaccurate model forms are developed; one that underestimates the shear area coefficient and one that overestimates the shear area coefficient. Furthermore, the model developer is

assumed to be unaware of the true values of K_1 and K_2 shown in Figure 4.1. Therefore, the two inexact models will inaccurately account for the shear deformations, while all three models will remain uncertain as to which values of K_1 and K_2 are appropriate for the analysis. These inaccurate and imprecise models will thus result in unavoidable disagreements between predictions and experiments.

4.1 Exact Model

The portal frame is constructed from vertical columns that sit on pinned supports, while the beams are rigidly connected to the columns at two levels except at the connections of the left and center first story columns to the left, first story beam. Here, the connections are represented with linear rotational springs. All members of the portal frame have uniform cross-sections. A static, external horizontal load is applied to the top of the portal frame, and the members are oriented in such a way that they bend about their strong axis. The applied force is assumed to be in the elastic range and the sections are assumed not to yield under bending or shear stresses. Geometric data and material properties of the model frame are provided in Table 4.1.

Table 4.1: Input values for the portal frame

Property Description	**Beams**	**Columns**
Member Length (m)	4	3
Cross-Sectional Area (m^2)	0.05	0.05
Moment of Inertia (m^4)	0.1	0.05
Young's Modulus (Pa)	200x10^1	200x10^1
Shear Area Coefficient	0.95;1;1.05	0.95;1;1.05
Poisson's Ratio	0.3	0.3

Here, Timoshenko beam theory (Hartmann and Katz 2007) is applied to consider the axial, shear, and flexural deformations of the frame elements. All members are assumed to experience zero deformations when not under loading; i.e., gravitational loads due to self-weight are neglected.

Synthetic experimental data is generated by applying a known horizontal force to the top story of the portal frame and using a finite element model to solve for lateral displacements at six locations on the frame using a so-called "exact" model. This model is assumed to implement physically accurate assumptions and equations for determining shear deformations, while also using the "precise" values of K_1 and K_2. Experimental uncertainty is neglected for this application.

4.2 Accurate Model with Imprecise Input Parameters

The proposed model updating methodology is first demonstrated on an accurate model with imprecise parameter values of K_1 and K_2. In this study, to simulate the uncertainty in the stiffness parameters, Monte Carlo simulations are employed for the unknown values of K_1 and K_2. Here, a uniformly distributed range of values is specified for both K_1 and K_2. The ranges of values for both parameters are given in Table 4.2, and were selected as such so that all plausible values of K_1 and K_2 would be sampled. As mentioned in Chapter 2, the Monte Carlo method samples numerous random values from the specified ranges and evaluates the finite element model for each sampled pair of K_1 and K_2 to obtain model predictions. The model predictions are then compared to the synthetic experimental data to calculate the prediction error R for the various values of K_1 and K_2. Failure surfaces are then generated for the varying levels of R. Herein, R is

formulated as the absolute mean value of the normalized error between the synthetic experimental displacement data and the model predictions as follows:

$$\left\{ R = \left| \frac{\sum_{i=1}^{n} \left| \frac{y_{o_i} - y_{p_i}}{\max y_{o_i}} \right|}{n} \right| \qquad i = 1,2,\dots,n \right\} \qquad \text{(Equation 11)}$$

where n is the number of locations on the portal frame at which displacement measurements are taken, while y_o and y_p still represent the experimental measurements and model simulations, respectively. It should be noted that model fidelity still has an inverse relationship with the error calculated in Equation 11. The exact values for K_1 and K_2 as well as their ranges for the Monte Carlo predictions are provided in Table 4.2.

Table 4.2: Exact Values and Simulation Ranges for Input Parameters K_1 and K_2

	K_1	**K_2**
Exact Value	33000	40000
Lower Bound	3300	4000
Upper Bound	132000	160000

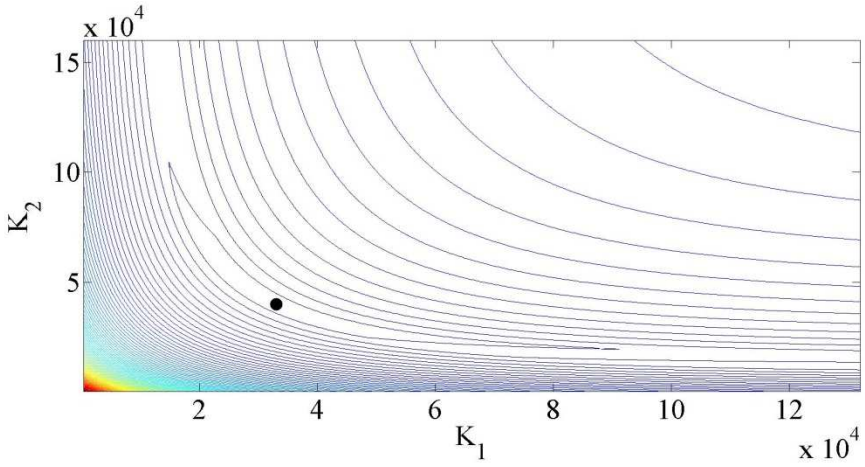

Figure 4.2: Two-dimensional representation of the expanding failure surfaces for the accurate model with imprecisely known input parameters, where the black dot represents the location of the nominal parameter values

The dot in Figure 4.2 represents the exact values of the input parameters K_1 and K_2. The formation of the failure contours and their increasing size can be seen in the figure. The model form used in the development of this figure was the "accurate" model form, and that is why the failure contours are centered on the true parameter values. A three dimensional representation of the failure surfaces as they expand with increasing prediction error is shown in Figure 4.3.

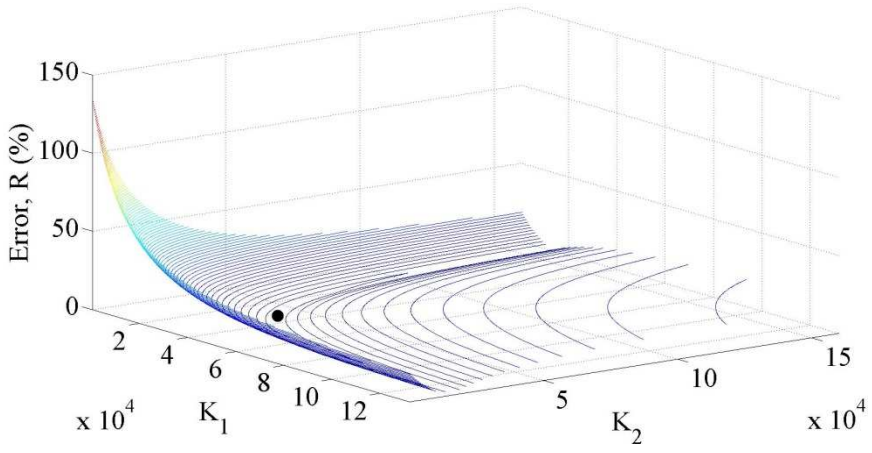

Figure 4.3: Three-dimensional representation of the failure surfaces for the accurate model

Figure 4.3 illustrates the relationship between the error in the model output (i.e. lack of fidelity) and the size of the domain of parameter values encompassed by the failure surface. As expected, the domain of acceptable parameter values encompassed by each failure surface increases with increasing error in the model output. It can be seen that the contours increase in size quite rapidly, suggesting that the model possibly has a favorable trade-off between fidelity and robustness. It can also be seen that the error in predictions increases very rapidly for small values of K_1 and K_2, which is expected. As the values of K_1 and K_2 approach zero, the frame becomes unstable and thus yields large lateral deformations. On the other hand, for very large values of K_1 and K_2, the frame becomes stiffer and asymptotically converges to having fully rigid columns. Thus, the increase in discrepancy between predictions and experiments develops much more slowly. This relationship is depicted in Figure 4.4.

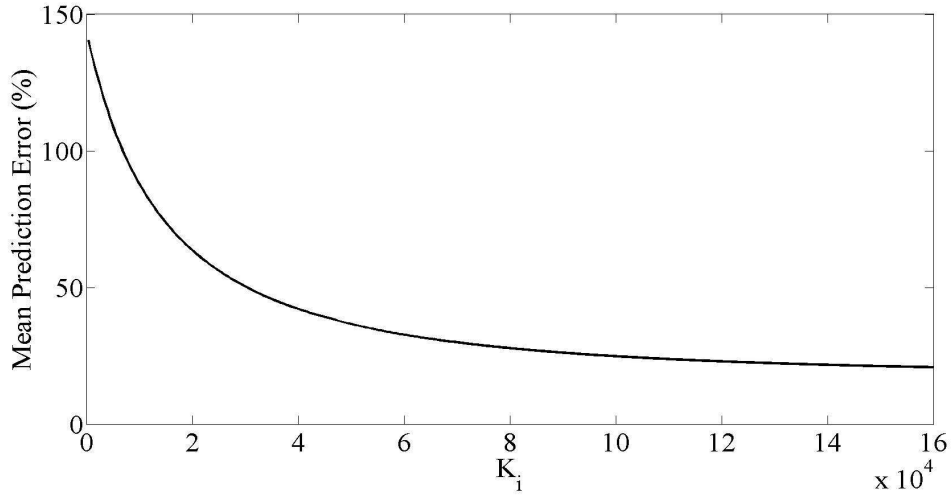

Figure 4.4: Relationship between increasing connection stiffness (K_i) and the mean prediction error

Moreover, as the model form changes, shifts in the origin of the failure contours would be expected. This shift is due to the introduction of model bias and/or compensating effects between the uncertain parameters into the prediction results.

4.3 Inexact Models with Uncertain Input Parameters

In this study, the two inaccurate finite element models that are used to analyze the portal frame displacements are assumed to underestimate and overestimate the shear area coefficients necessary to incorporate the shear deformation by 5% in both models (i.e., 95% of the shear area and 105% of the shear area, respectively) in the element stiffness matrices, therefore, introducing two different model forms. This will unavoidably introduce imperfections into the models ultimately changing each model's behavior. The failure surfaces for the two inexact models are generated and shown in Figures 4.5 and 4.6.

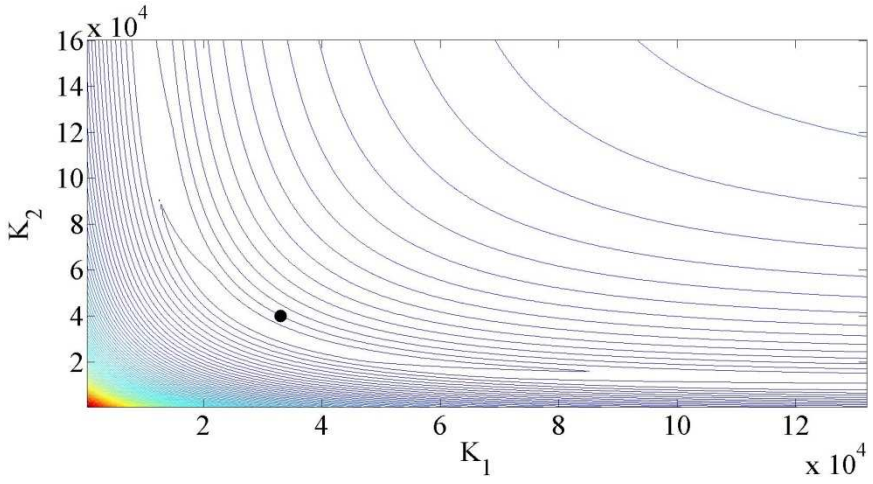

Figure 4.5: Two-dimensional failure surfaces for the inexact model with 95% shear deformations

As seen in Figure 4.5, the underestimation of the shear area causes the failure surfaces to shift downward, which is evident when compared to Figure 4.2. As shown, the nominal parameter values represented by the black dot in the figure no longer fall at the center of the initial (smallest) failure surface. This shift is a result of the compensations between model imperfections and uncertain input parameters. This entails that the model requires lower values of K_1 and K_2 to increase the lateral deformations of the frame since less shear deformations are accounted for due to less shear area. As expected, the opposite effect is seen in Figure 4.6 for the inexact model that is overcompensating for shear deformations.

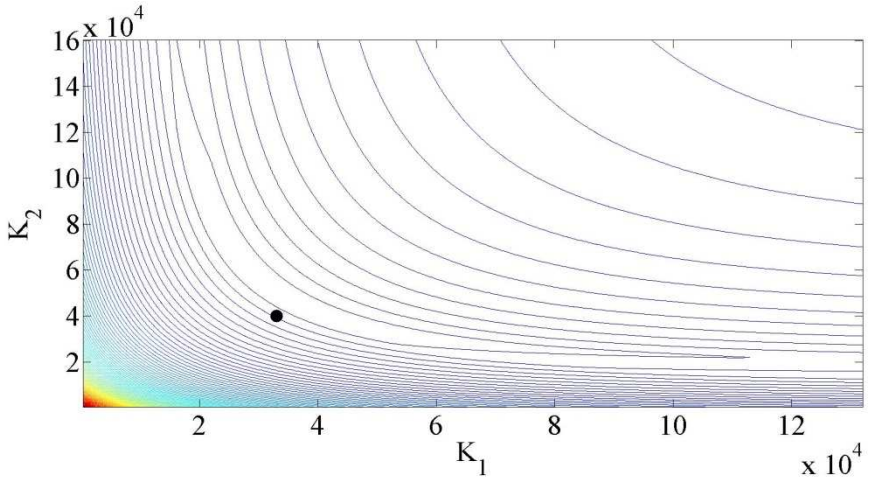

Figure 4.6: Two-dimensional representation of failure surfaces for 105% shear deformations

In Figure 4.6, the compensating effects caused by the imprecision in the model due to overcompensation of shear deformations causes an upward shift in the failure surfaces, encompassing larger values of K_1 and K_2. Referring back to Figure 4.4, the larger stiffness values create stiffer connections and, therefore, decrease the model's calculated lateral displacements and, in turn, the prediction error. It can also be seen that the initial failure surface is larger than that of the two previous models, meaning that this model can allow for more variations in the parameter values for this level of fidelity.

4.4 Utilizing the Failure Surfaces

The failure surfaces for the three models are evaluated for their probability of successfully satisfying the fidelity threshold values. Here, the unbounded sets of input parameter values are centered at the nominal parameter values, which in this study are the exact values of K_1 and K_2 used in the formulation of the exact model and also given in

Table 4.2. For each fidelity threshold value evaluated, the uncertainty parameter α is increased from 0-100% of its original size at steps of 20%. The original size of α is set as $[(K_i-K_i*0.125),(K_i+K_i*0.125)]$. Thus, an α value of zero indicates this initial range. Fidelity thresholds are evaluated between 0.01-1.41% error. Figures 4.7, 4.8 and 4.9 show a single failure surface from each of the three models being compared to a set of parameter values for K_1 and K_2 of a certain size.

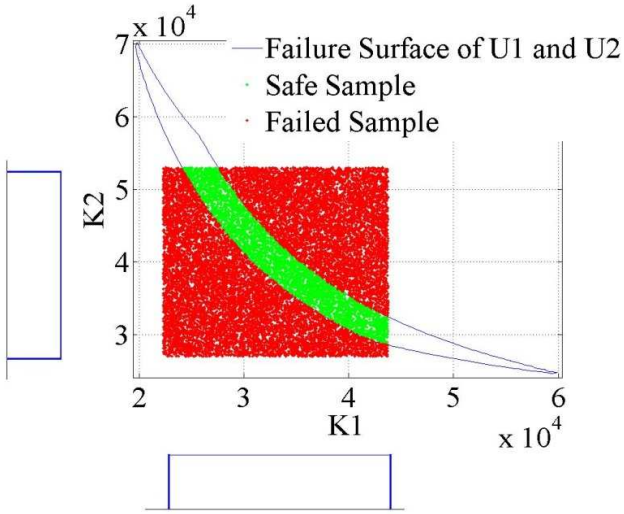

Figure 4.7: Failure surface for the accurate model at *R* = 0.885% being evaluated for α = 40%

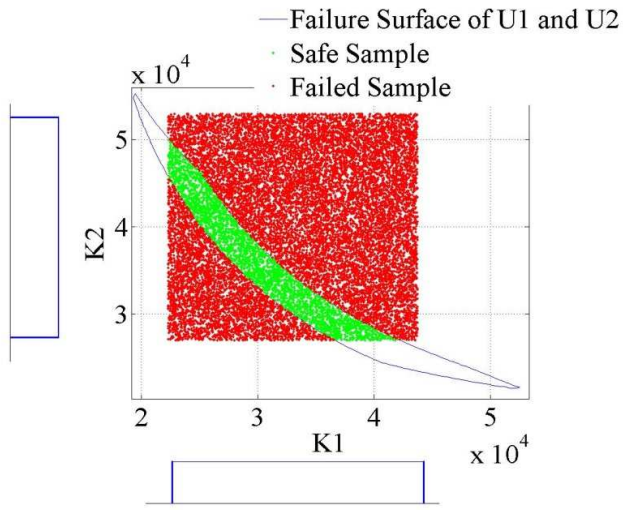

Figure 4.8: Failure surface for the inexact model accounting for 95% shear deformations at R = 0.885% being evaluated for α = 40%

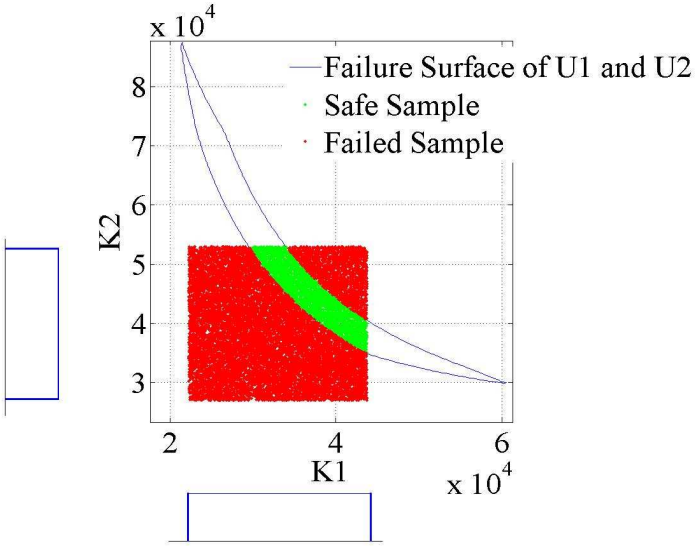

Figure 4.9: Failure surface for the inexact model accounting for 105% shear deformations at R = 0.885% being evaluated for α = 40%

By comparing the failure surfaces in Figures 4.7, 4.8 and 4.9, it can be seen that their sizes and locations differ for all three models. Given that these failure surfaces are all associated with the same fidelity threshold R_t = 0.885%, this proves the existence of multiple model forms that can satisfy the same fidelity requirement. However, from the method proposed in this manuscript, it can also be seen how the utilization of the failure surfaces distinguishes between the models even though all three still satisfy the same fidelity threshold. The area of the parameter set that falls within the failure surface represents each model's ability to satisfy that fidelity requirement. Figures 4.10, 4.11 and 4.12 display the interaction between increasing prediction error and increase uncertainty parameter and their effect on each model's probability of successfully satisfying the fidelity threshold.

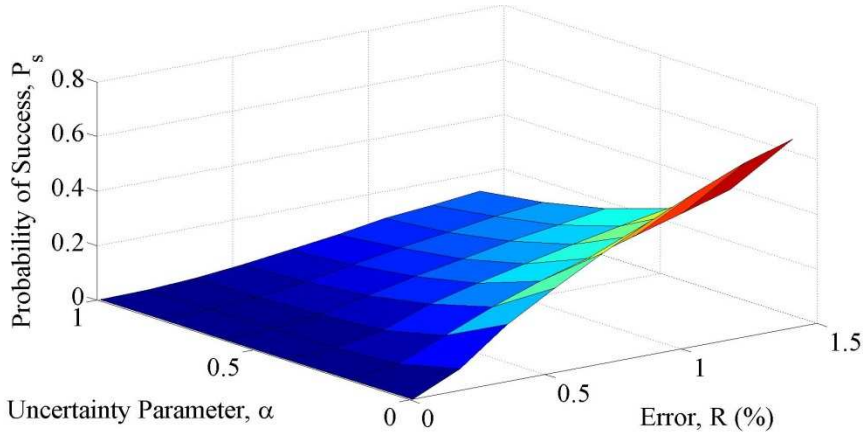

Figure 4.10: Three-dimensional plot of probability of success versus the uncertainty parameter versus prediction error (inverse of fidelity) for the accurate model

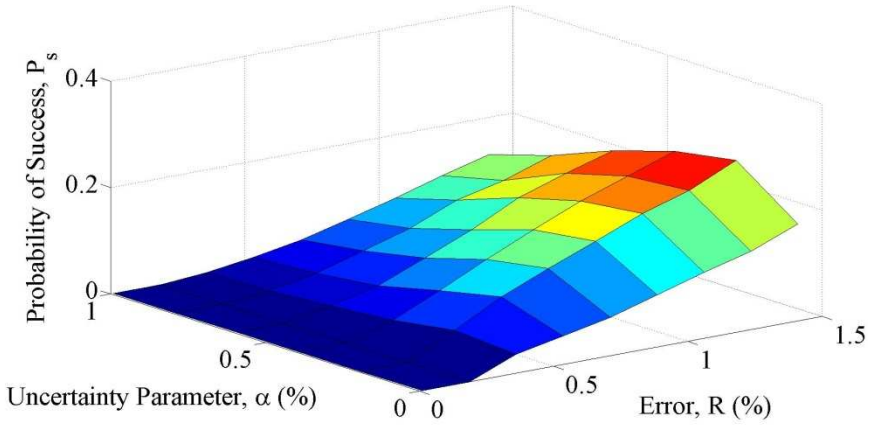

Figure 4.11: Three-dimensional plot of probability of success versus the uncertainty parameter versus prediction error (inverse of fidelity) for the model with 95% shear deformations

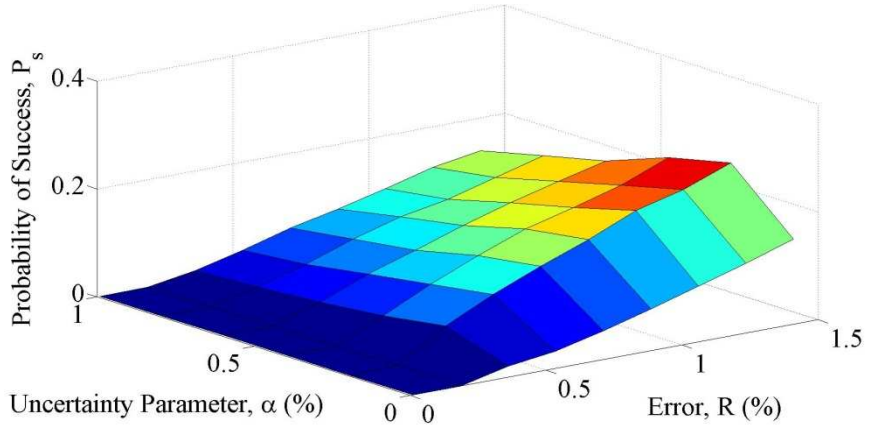

Figure 4.12: Three-dimensional plot of probability of success versus the uncertainty parameter versus prediction error (inverse of fidelity) for the model with 95% shear deformations

Figure 4.10 illustrates the trade-off between the fidelity, uncertainty parameter and probability of success. In this figure, one cannot improve the probability of success without decreasing the uncertainty parameter and/or decreasing the model fidelity (i.e., increasing prediction error). These attributes are said to be antagonistic and are the reason that the model developer is also a decision maker.

Figures 4.11 and 4.12 display these antagonistic trade-offs between the three attributes except for a small region in both figures (the far right side of both figures) where the antagonistic traits do not hold true. This can occur when model bias and compensating effects between model parameters cause the failure surface to shift away from the nominal parameter values, as shown in Figures 4.5 and 4.6. In this situation, when the unbounded nested sets are applied to the increasing failure surfaces, only the extreme values of a set fall within the failure surface, yielding a small probability of success. However; the successive sets, which are larger than the previous sets contain more values that fall within the failure surface and, thus, yield a larger probability of success. Therefore, with increasing uncertainty in the input parameters, the model's probability of successfully satisficing the fidelity requirement increases.

Given these three figures, it can be seen that the accurate model in Figure 4.10 displays more favorable trade-offs in that its probability of success increases more quickly than the other two models. Though this may seem intuitive, it does signify that the proposed method is effective in helping the model developer identify the model that best represents the physical experiment, even in the face of parametric uncertainty. This is further illustrated in Figures 4.13, 4.14 and 4.15.

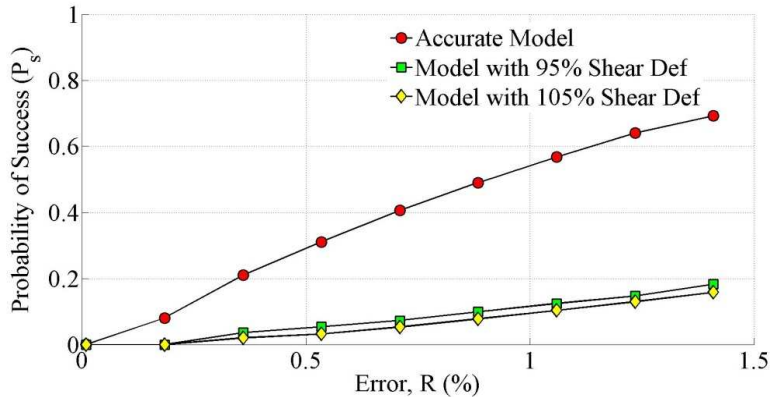

Figure 4.13: Probability of Success versus Prediction Error for a constant α

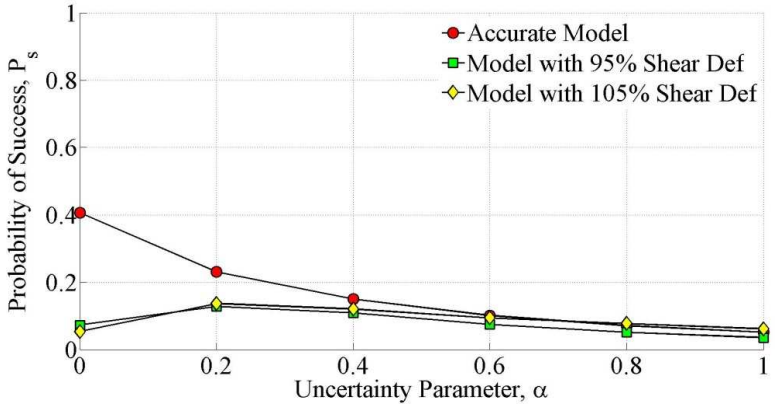

Figure 4.14: Probability of Success versus the uncertainty parameter for constant R

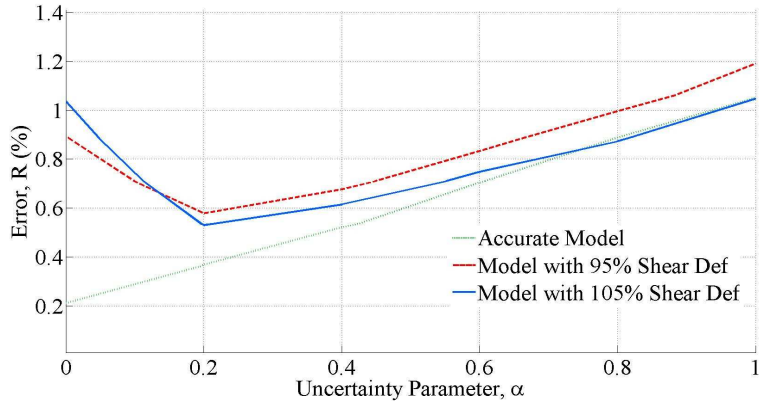

Figure 4.15: Prediction error (inverse of fidelity) versus the uncertianty parameter for a constant P_s

Figure 4.13 shows that the probability of successfully satisfying the fidileity requirements for the accurate model increases much faster than the two inexact models given a constant value of the uncertainty parameter. In this figure, the value of the uncertainty parameter is zero, which means that the initial set range of parameter values was used for evaluation.

From Figure 4.14, it can be seen that as the uncertinaty parameter is allowed to expand, and the probability of success for all three models begins to converge. This means that the differences in model form are more distinguishable for lower values of input parameter uncertainty. Once a sufficient amount of uncertainty is allowed in the input parameters, the compensations between the bias errors and parameter uncertainties allow the two inaccurate models to yield a probability of success similar to that of the accurate model.

Figure 4.15 compares the fidelity and the uncertianty parmaeter for a single probability of success. Here, the decision maker can establish a minimum probability of success requirement and then evaluate which model performs best given the increasing uncertianty in input parameters. The common factor in all three figures is that the decision maker must be able to decide upon the *threshold values* to be able to make informed decisions. The following section explains the use of an optimization algorithm to assist in this process.

CHAPTER FIVE

MODEL EVALUATION USING MULTI-OBJECTIVE OPTIMIZATION

The approach discussed in Chapter 3 and demonstrated in Chapter 4 on a case study application of a steel portal frame for model selection naturally leads to a multi-objective optimization problem with three distinct objectives: fidelity, uncertainty in input parameters and probability of success of satisfying the fidelity with a given amount of uncertainty in the input parameters. As reported earlier, these three objectives tend to be uncooperative in nature, and thus a single solution that optimizes all of these objectives does not always exist in the solution space. However, a set of solutions that are better than all other solutions can be obtained.

Unlike single objective optimization, the purpose of which is to search for a single best design, multi-objective optimization yields a family of optimum designs, which is to find multiple Pareto-optimal solutions. When the objectives are conflicting (or uncooperative), it is not possible to have a single solution which simultaneously optimizes all objectives (Deb et al. 2002). However, a set of solutions, referred to as Pareto front that are better than all other solutions can be obtained. These designs constitute a Pareto optimum set (or Pareto front), as illustrated in Figure 5.1.

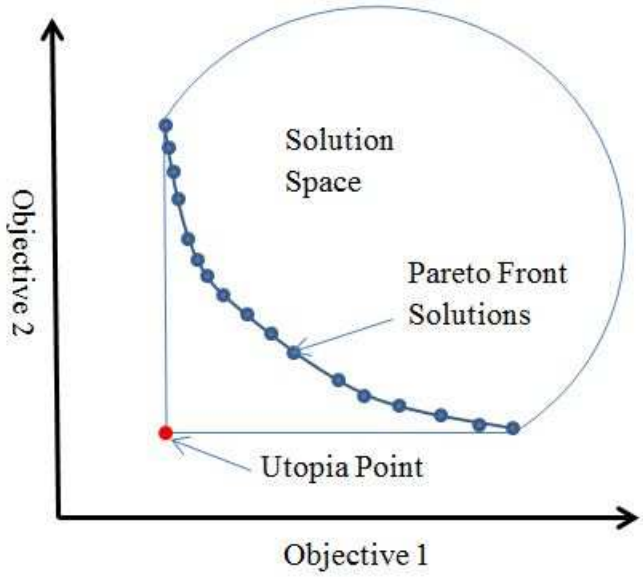

Figure 5.1: Illustration of a Pareto Front

A general multi-objective optimization problem can be expressed as:

$$\text{Minimize: } \mathbf{F}(\mathbf{d}) = \left[f_1(\mathbf{d}), f_2(\mathbf{d}), \ldots, f_l(\mathbf{d}) \right]$$
$$\text{Subject to: } g_i(\mathbf{d}) \leq 0 \quad i = 1, \ldots, n \qquad \text{(Equation 12)}$$

with f representing each of the single objective functions, and g representing the constraint functions. The Pareto front can be viewed as a set of designs, which dominate all other designs (Marler and Arora 2004). The domination relationship is defined as follows:

- design B is dominated by design A, if A is superior to B in at least one criteria (i.e., $f_i(d)A < f_i(d)B$ for at least one i), and
- A is not inferior to B in all other criteria (i.e., $f_i(d)A \leq f_i(d)B$ for all other i). A design that is not dominated by any other design is included in the Pareto front

Thus, the Pareto front supplies a clear, visual representation of the trade-off between multiple objectives as, among the Pareto front solutions, one cannot gain improvement in one of the objectives without compromising the other objective(s).

Many multi-objective optimization methods can also be implemented to derive the Pareto front such as MOEAs, Zitzler and Thiele's (1998) strength Pareto EA (SPEA), Knowles and Corne's (1999) Pareto-archived evolution strategy (PAES), and Rudolph's (1997) elitist GA. Over the past decade, a number of evolutionary algorithms (MOEAs) have also been suggested to solve such multi-objective problems (Fonseca and Fleming 1993; Hom et al. 1994; Srinivas and Deb 1994). Among the evolutionary algorithms, the low computational requirements, its elitist approach and parameter-less sharing make Non-dominated Sorting Genetic Algorithm (NSGA-II) a widely-used algorithm (Deb et al. 2002).

Herein, NSGA-II is employed to solve the proposed multi-objective model selection problem introduced in Chapter 4 considering, first, probability of success and fidelity of the prediction obtained with the nominal parameter values, and then, second, all three objectives. The two-objective optimization will yield a line of optimal solutions that separates two areas; one area containing feasible solutions and the other containing infeasible solutions. The three-objective optimization yields a three-dimensional surface of solutions which separates two volumes, again one feasible and the second, infeasible. A population size of 50 is used for each generation, and the converged solution (i.e., Pareto front) is acquired after 100 generations.

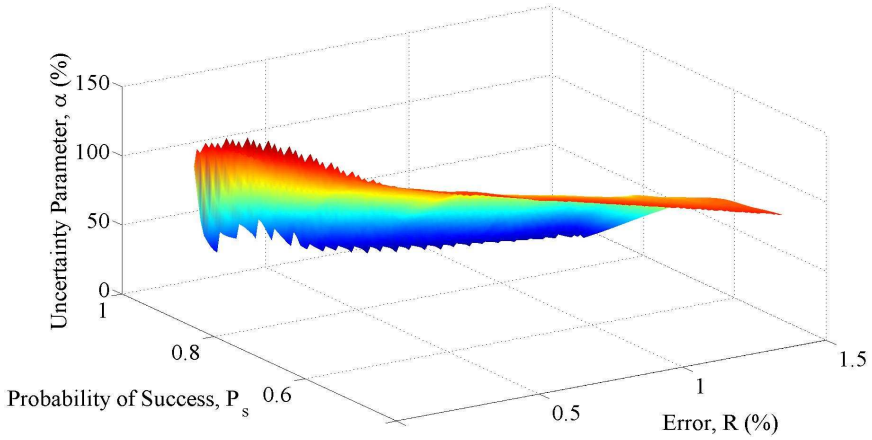

Figure 5.2: Evaluation of the accurate model through multi-objective optimization considering fidelity (error), uncertainty (α) and probability of success

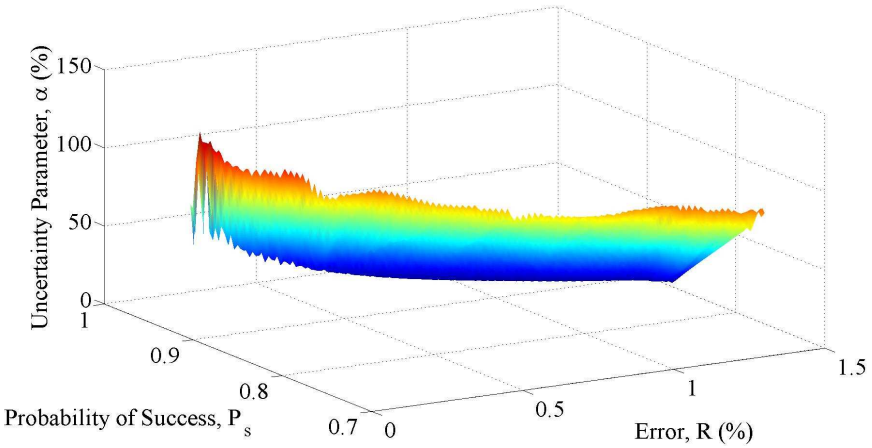

Figure 5.3: Evaluation of the inaccurate model through multi-objective optimization considering fidelity (error), uncertainty (α) and probability of success

As shown in Figure 5.2, as the uncertainty parameter increases in magnitude the optimal solutions only exist for lower probabilities of success. Also, more optimal solutions exist for high levels of error (low fidelity) as well. The surfaces shown in Figures 5.2 and 5.3 not only represent the optimal solutions to the multi-objective

problem, but they also separate feasible solutions from infeasible solutions. Less optimal, but feasible, solutions exist above and behind the surfaces, while infeasible solutions would exist below the surfaces. This is due to the antagonistic qualities between the three objectives.

By comparison of Figures 5.2 and 5.3, one can see that the Pareto front surface of the accurate model in Figure 5.2 obtains more solutions with low error (high fidelity) and high uncertainty. This, in turn, translates to a more robust model. Also, it can be seen that the accurate model contains higher probability of success solutions. As a DM, the evaluation of these three attributes yields a clear model choice of the accurate model.

CHAPTER SIX

CONCLUSION

In numerical modeling, uncertainties inherently exist due to unknown or partially known values of input parameters as well as an imperfect understanding or lack of knowledge of the underlying physics that drive the model. These uncertainties often lead to compensating effects between the input parameters that may give the modeler a false perception of the accuracy of the model. Compensating effects between input parameters typically result in the existence of non-unique solutions. Although we acknowledge that the existence of a "perfect" model is highly unlikely, it is necessary to implement criteria that adequately distinguish between the robustness of multiple model forms with varying domains of acceptable input parameter which satisfy the same fidelity threshold value. At the same time the criteria cannot be overly conservative leading to unrealistic, over-designed systems. Therefore, the method presented in this manuscript assesses different model forms based on three criteria: fidelity-to-data, robustness-to-uncertainty, and probability of successfully satisfying a predefined fidelity threshold requirement.

In this manuscript, a new methodology is proposed for assessing the robustness of a simulation model to discriminate between multiple models that yield similar predictions. Instead of estimating the boundary of solutions which satisfy a given level of information, the proposed approach implements an optimization algorithm which solves for the exact boundary of solutions that satisfy a given level of prediction fidelity, or otherwise known as the inverse error of the predictions. This boundary is referred to as the model's failure surface. By accurately defining the failure surface, the modeler can

then exploit this domain by spatially comparing the contained parameter values with increasing sets of the modeler's best estimation of the real parameter values. These sets of parameter values are unbounded, monotonically increasing sets of values whose size are defined by a metric known as the uncertainty parameter α. The increasing magnitude of α represents increasing the uncertainty in the parameter values. A spatial comparison refers to comparing the parameter values contained in the failure surface to those contained in the increasing input parameter sets.

The goal of this procedure is to quantify how the model reacts to uncertainty in the input parameters, also known as the model's robustness to uncertainty. Therefore, the ratio of the number of parameter values from the set that fall within the failure surface domain to the total number of parameter values in the set is used as the metric to quantify this relationship. In this manuscript, this measure is known as the probability of success. More specifically, it is the probability of the model to successfully satisfy the fidelity threshold value associated with a particular failure surface. Thus, this method defines three metrics that are used by the model developer to decide upon the most appropriate model form, the model fidelity, uncertainty parameter and probability of success. To highlight the conflicting relationships between these metrics, a multi-objective optimization procedure is performed using a non-dominated genetic sorting algorithm known as NSGA-II. From these results, a modeler can make an informed decision as to which model form best characterizes the realistic phenomenon being simulated.

REFERENCES

Srinivas, N., and Kalyanmoy Deb. 1994. “Muiltiobjective Optimization Using Nondominated Sorting in Genetic Algorithms.” Evol. Comput. 2 (3) (September): 221–248.

Horn, Jeffrey, Jeffrey Horn, Nicholas Nafpliotis, Nicholas Nafpliotis, David E. Goldberg, and David E. Goldberg. 1994. “A Niched Pareto Genetic Algorithm for Multiobjective Optimization.” In In Proceedings of the First IEEE Conference on Evolutionary Computation, IEEE World Congress on Computational Intelligence, 82–87.

Fonseca, Carlos M., and Peter J. Fleming. 1993. Genetic Algorithms for Multiobjective Optimization: Formulation, Discussion and Generalization.

Rudolph, Günter. 1997. Convergence Properties of Evolutionary Algorithms. Kovac.

Knowles, J., and D. Corne. 1999. “The Pareto Archived Evolution Strategy: a New Baseline Algorithm for Pareto Multiobjective Optimisation.” In Proceedings of the 1999 Congress on Evolutionary Computation, 1999. CEC 99, 1:-105 Vol. 1.

Marler, R. T., and J. S. Arora. 2004. “Survey of Multi-objective Optimization Methods for Engineering.” Structural and Multidisciplinary Optimization 26 (6) (April 1): 369–395.

Deb, K., A. Pratap, S. Agarwal, and T. Meyarivan. 2002. “A Fast and Elitist Multiobjective Genetic Algorithm: NSGA-II.” IEEE Transactions on Evolutionary Computation 6 (2):

Hartmann, Friedel, and Casimir Katz. 2007. Structural Analysis with Finite Elements. Springer.

Farajpour, I., and S. Atamturktur. 2013. “Partitioned Analysis of Coupled Numerical Models Considering Imprecise Parameters and Inexact Models.” Journal of Computing in Civil Engineering 0 (ja): null.

Atamturktur, S., F.M. Hemez, and J.A. Laman. 2012. “Uncertainty Quantification in Model Verification and Validation as Applied to Large Scale Historic Masonry Monuments.” Engineering Structures 43 (October): 221–234.

Kennedy, Marc C., and Anthony O’Hagan. 2001. “Bayesian Calibration of Computer Models.” Journal of the Royal Statistical Society. Series B (Statistical Methodology) 63 (3) (January 1): 425–464.

Draper, David. 1995. “Assessment and Propagation of Model Uncertainty.” Journal of the Royal Statistical Society. Series B (Methodological) 57 (1) (January 1): 45–97.

Ben-Haim, Yakov, and François M. Hemez. 2012. “Robustness, Fidelity and Prediction-looseness of Models.” Proceedings of the Royal Society A: Mathematical, Physical and Engineering Science 468 (2137) (1–8): 227–244.

Chen, W., M. M. Wiecek, and J. Zhang. 1999. “Quality Utility—A Compromise Programming Approach to Robust Design.” Journal of Mechanical Design 121 (2) (June 1): 179–187.

Hampel, Frank R. 1971. “A General Qualitative Definition of Robustness.” The Annals of Mathematical Statistics 42 (6) (December): 1887–1896.

Y. Ben-Haim. 2006. Info-gap Decision Theory Decisions Under Severe Uncertainty. Oxford: Academic.

Mulvey, John M., Robert J. Vanderbei, and Stavros A. Zenios. 1995. “Robust Optimization of Large-Scale Systems.” Operations Research 43 (2) (March 1): 264–281.

Lee, Kwon-Hee, and Gyung-Jin Park. 2001. “Robust Optimization Considering Tolerances of Design Variables.” Computers & Structures 79 (1) (January): 77–86.

Renaud, J. E. 1997. “Automatic Differentiation in Robust Optimization.” AIAA Journal 35 (6) (June): 1072–1079.

Chen, Wei, Janet K. Allen, Kwok-Leung Tsui, and Farrokh Mistree. 1996. “A Procedure For Robust Design: Minimizing Variations Caused By Noise Factors And Control Factors.” ASME Journal of Mechanical Design 118: 478–485.

Parkinson, A., C. Sorensen, and N. Pourhassan. 1993. “A General Approach for Robust Optimal Design.” Journal of Mechanical Design 115 (1) (March 1): 74–80.

Ben-Haim, Yakov. 1995. “A Non-probabilistic Measure of Reliability of Linear Systems Based on Expansion of Convex Models.” Structural Safety 17 (2) (August): 91–109.

Ben-Haim, Yakov. 1996. Robust Reliability in the Mechanical Sciences. Springer.

Ben-Haim, Yakov, and Isaac Elishakoff. 1990. Convex Models of Uncertainty in Applied Mechanics. Elsevier.

Ben-Haim, Yakov. 1994. “Convex Models of Uncertainty: Applications and Implications.” Erkenntnis 41 (2) (September 1): 139–156.

Moens, David, and Dirk Vandepitte. 2005(b). “A Survey of Non-probabilistic Uncertainty Treatment in Finite Element Analysis.” Computer Methods in Applied Mechanics and Engineering 194 (12–16) (April 8): 1527–1555.

Elton, David J., C. Hsein Juang, and Ping-Sien Lin. 2000. “Vertical Capacity of Piles Using Fuzzy Sets.” Civil Engineering and Environmental Systems 17 (3): 237–262.

Zadeh, L.A. 1965. “Fuzzy Sets.” Information and Control 8 (3) (June): 338–353.

Dubois, Didier. 2006. “Possibility Theory and Statistical Reasoning.” Computational Statistics & Data Analysis Vol: 47–69.

Moens, David, and Dirk Vandepitte. 2005(a). “A Fuzzy Finite Element Procedure for the Calculation of Uncertain Frequency-response Functions of Damped Structures: Part 1—Procedure.” Journal of Sound and Vibration 288 (3) (December 6): 431–462.

Qiu, Z., & Wang, X. (2003). Comparison of dynamic response of structures with uncertain-but-bounded parameters using non-probabilistic interval analysis method and probabilistic approach.*International Journal of Solids and Structures,40*(20), 5423–5439.

Rao, S. S., and L. Berke. 1997. “Analysis of Uncertain Structural Systems Using Interval Analysis.” AIAA Journal 35 (4) (April): 727–735.

Pepin, J. E., Rodriguez, E. A., Thacker, B. H., & Riha, D. S. (2001). Probabilistic structural response with geometric shape uncertainties under collapse loading. In *IMAC-XIX: A Conference on Structural Dynamics,* (Vol. 2, pp. 1332–1338).

Hills, Richard G., and Timothy G. Trucano. 1999. “Statistical Validation of Engineering and Scientific Models: Background.” Sandia National Laboratories, SAND99-1256: 36

Wu, Y.-T., H. R. Millwater, and T. A. Cruse. 1990. “Advanced Probabilistic Structural Analysis Method for Implicit Performance Functions.” AIAA Journal 28 (9) (September): 1663–1669.

Hemez, François M., and Yakov Ben-Haim. 2004. “Info-gap Robustness for the Correlation of Tests and Simulations of a Non-linear Transient.” Mechanical Systems and Signal Processing 18 (6) (November): 1443–1467.

Taguchi, Genichi. 1993. “Robust Technology Development.” Mechanical Engineering-CIME, March.

Phadke, Madhav Shridhar. 1989. Quality Engineering Using Robust Design. Englewood Cliffs, N.J: Prentice Hall.

Au, F.T.K., Y.S. Cheng, L.G. Tham, and G.W. Zeng. 2003. “Robust Design of Structures Using Convex Models.” Computers & Structures 81 (28–29) (November): 2611–2619.

XiaopingDu, and WeiChen. 2012. “Efficient Uncertainty Analysis Methods for Multidisciplinary Robust Design”. Research-article. May 17.

Belegundu, A. D., and Shenghua Zhang. 1992. “Robustness of Design Through Minimum Sensitivity.” Journal of Mechanical Design 114 (2) (June 1): 213–217.

Elishakoff, I. 1995. “Essay on Uncertainties in Elastic and Viscoelastic Structures: From A. M. Freudenthal’s Criticisms to Modern Convex Modeling.” Computers & Structures 56 (6) (September 17): 871–895.

Berman, A. (1995). Multiple acceptable solutions in structural model improvement. AIAA Journal, 33(5), 924–927.

Oberkampf, William L., and Matthew F. Barone. 2006. Measures of Agreement Between Computation and Experiment: Validation Metrics.

Doebling, Scott W. 2002. “Structural Dynamics Model Validation: Pushing the Envelope”. LA-UR-02-2200. Los Alamos National Lab., NM (US).

Lassmann, K. (1992). TRANSURANUS: a fuel rod analysis code ready for use. J. Nucl. Mater., 188,295-302

Koh, C. G. and Kelly, J. M. (1990), Application of fractional derivatives to seismic analysis of base-isolated models. Earthquake Engng. Struct. Dyn., 19: 229–241.

Atamturktur, S., Hemez, F., Williams, B., Tome, C., & Unal, C. (2011). A forecasting metric for predictive modeling. Computers & Structures, 89(23–24), 2377–2387.